

Doctoral Dissertation

**STUDY ON STRENGTH EVALUATION AND STRUCTURAL
ANALYSIS FOR SPHERICAL PRESSURE SHELLS SUBJECTED
TO EXTERNAL PRESSURE**

September 2021

**Graduate School of Marine Science and Technology
Tokyo University of Marine Science and Technology
Doctoral Course of Applied Marine Environmental Studies**

HUANG YUNGHSIN

Doctoral Dissertation

**STUDY ON STRENGTH EVALUATION AND STRUCTURAL
ANALYSIS FOR SPHERICAL PRESSURE SHELLS SUBJECTED
TO EXTERNAL PRESSURE**

September 2021

**Graduate School of Marine Science and Technology
Tokyo University of Marine Science and Technology
Doctoral Course of Applied Marine Environmental Studies**

HUANG YUNGHSIN

Abstract

With the improvement of ocean exploration and technological advances, the deep submergence vehicle (DSV) has played a crucial role in underwater survey activities. The DSVs are divided into three types: autonomous underwater vehicles, remotely operated vehicles, and human occupied vehicle (HOVs). Among them, the HOV has the most complex design and manufacturing processes. The spherical pressure shell is the main structure of the HOV, and it provides safe living space for scientists and investigators. This pressure shell plays a crucial role in human occupied vehicles; therefore, it should be designed precisely and its ultimate strength should be analyzed.

This thesis uses five pressure shells as design targets and recalculates them using seven classification rules. However, according to the design results of this thesis, there are significant differences in the design results of various classification rules; however, in fact, the design methods of classification rules have not been discussed and unified. According to the results obtained herein and based on the consideration of various classification rules, the maximum deviation between the calculated and actual thickness values is approximately 30%.

The elastic-plastic buckling analysis was performed with the Riks method in ABAQUS to confirm the ultimate strength. It is demonstrated that the results calculated by LR rules are more stable and smaller deviations than other rules.

LR rules divide the design method based on two collapse problems. In the first stage, when thickness/radius ratio is small, the pressure shell mainly collapses due to buckling. Generally thin spherical shells belong to the first stage. In the second stage, as thickness/radius ratio increases, the pressure shell mainly collapses due to yielding, which means that the stresses in the spherical shell reach the yield strength of the material. In the LR rules, material coefficients are considered when evaluating structural stability. Using the design correction curve of the British Standards Institution for the correction of the yield load shows that the thickness of the pressure shell is significantly lower than that of the original design. Despite the fact that the thickness is reduced, the structural strength can be maintained within a safe range that meets the design requirements.

This thesis mainly focuses on the design results obtained based on the various classification rules and proposes a design method to estimate the scantling of spherical pressure shells. This method can reduce the waste of design time and

reduce estimation errors. Since the actual pressure shells are assembled by bending and welding, it is inevitable that initial imperfections and residual stresses will inevitably occur during the production process, and the actual strength of pressure shells will be reduced from the theoretical value. The design method proposed by this thesis institute also discussed this initial imperfections, and brought the design results closer to the actual situation.

Although this method has yielded good design results in the five pressure shells tested herein, there are several openings in the spherical pressure shell that weaken its critical strength. In future research, an in-depth study of the opening reinforcement method based on the design method proposed by this thesis.

Keywords: Ocean engineering, Spherical pressure shell, Classification rules, Strength evaluation, Ultimate strength, Initial imperfection, Numerical analysis

Contents

Abstract.....	I
Contents.....	III
List of Figures.....	VI
List of Tables.....	VII
List of Symbols and Abbreviations	VIII
Chapter 1 Introduction	1
1.1 Background.....	1
1.1.1 Overview of DSV	1
1.1.2 Spherical pressure shells of HOV	3
1.2 Motivation and innovations	5
1.3 Structure of the thesis	7
References	9
Chapter 2 Criteria and formulas	12
2.1 Introduction	12
2.2 Estimation method of classification society	14
2.2.1 DNVGL	14
2.2.2 Det Norske Veritas (DNV)	15
2.2.3 American Bureau of Shipping (ABS).....	16
2.2.4 Lloyd's Register of Shipping (LR)	17
2.2.5 Bureau Veritas (BV).....	17
2.2.6 Russian Maritime Register of Shipping (RS)	19
2.2.7 China Classification Society (CCS)	20
2.2.8 Nippon Kaiji Kyokai (NK)	21
2.3 BSI specification PD 5500	22
References	24

Chapter 3	Design of spherical pressure shells.....	25
3.1	Introduction	25
3.2	Design objects and material properties.....	25
3.3	Comparison of classification rules	26
3.4	Summary.....	28
	References	29
Chapter 4	Structural analysis	30
4.1	Introduction	30
4.2	ABAQUS software	30
4.3	FEA overview	31
4.2.1	Finite element modeling	33
4.2.2	Boundary conditions.....	37
4.2.3	Verification.....	38
4.4	Analysis of spherical pressure shell	41
4.4.1	The yield load analysis	41
4.4.2	The eigenvalue buckling anaysis.....	42
4.4.3	The elastic–plastic buckling analysis	45
4.5	Summary.....	49
	References	51
Chapter 5	Proposal	52
5.1	Discussion.....	52
5.2	Proposal of the pressure shell design.....	54
5.3	Results of the proposed design method	55
Chapter 6	Conclusions and future work.....	57
6.1	Conclusions	57
6.2	Future work	58
	Appendix	59

Appendix I Design of spherical pressure shell (Shinkai 6500)	59
Appendix II Design of spherical pressure shell (Alvin)	62
Appendix III Design of spherical pressure shell (Nautile)	65
Appendix IV Design of spherical pressure shell (Consul)	68
Appendix V Design of spherical pressure shell (Jiaolong)	71
Acknowledgment.....	74

List of Figures

Fig. 1-1 Remotely Operated Vehicle	2
Fig. 1-2 Autonomous Underwater Vehicle	2
Fig. 1-3 Human Occupied Vehicle	3
Fig. 1-4 Division of Roles of DSV	3
Fig. 1-5 Schematic Diagram of Spherical Pressure Shell.....	4
Fig. 1-6 Research Map of the Thesis	6
Fig. 2-1 Structural Imperfection Factor [7]	18
Fig. 2-2 Correction Curve of Elastic Buckling Load [7].....	19
Fig. 2-3 The coefficient C versus t/R_m [9].....	23
Fig. 2-4 Lower bound curve of the PD 5500 [12]	23
Fig. 3-1 Stress–Strain Curve of Ti-6Al-4V	26
Fig. 4-1 Process Chart Used for the Analysis of the Ultimate Strength	32
Fig. 4-2 Measured Schematic of the Out-of-circularity	33
Fig. 4-3 The Mesh Size Convergence Analysis Results	34
Fig. 4-4 Finite Element Model of Spherical Shell.....	37
Fig. 4-5 Loading Case and Boundary Conditions	38
Fig. 4-6 First-order Instability Mode of Shinkai 6500	43
Fig. 4-7 First-order Instability Mode of Alvin.....	44
Fig. 4-8 First-order Instability Mode of Nautille.....	44
Fig. 4-9 First-order Instability Mode of Consul	44
Fig. 4-10 First-order Instability Mode of Jiaolong.....	45
Fig. 4-11 Pressure Displacement Path Proposed by Shinkai 6500.....	46
Fig. 4-12 Pressure Displacement Path Proposed by Alvin	46
Fig. 4-13 Pressure Displacement Path of Nautille.....	47
Fig. 4-14 Pressure Displacement Path of Consul	47
Fig. 4-15 Pressure Displacement Path of Jiaolong.....	48
Fig. 5-1 Comparison Between P_y and P_e (Ti-6Al-4V ELI)	53
Fig. 5-2 Comparison Between P_y and P_e (Ti-6211).....	53
Fig. 5-3 Comparison Between P_y and P_e (Ti-6Al-4V)	54

List of Tables

Table 2-1 Coefficient of Reflecting Post Buckling Behavior (ψ).....	15
Table 2-2 Load Coefficient (γ)	16
Table 2-3 S Coefficient of Structural Slenderness (k).....	16
Table 3-1 Characteristics of the Existing Human Occupied Vehicles (HOVs)	25
Table 3-2 Material of the Existing Human Occupied Vehicles (HOVs)	26
Table 3-3 Material Properties	26
Table 3-4 Comparison of Actual Thickness and Design Thickness	27
Table 3-5 Comparison of Actual Thickness and Design Thickness (Continued).....	27
Table 3-6 Comparison of Actual Thickness and Design Thickness (Continued).....	27
Table 3-7 Comparison of Actual Thickness and Design Thickness (Continued).....	28
Table 4-1 Mesh Convergence Results of Shinkai 6500.....	34
Table 4-2 Mesh Convergence Results of Alvin	35
Table 4-3 Mesh Convergence Results of Nautile	35
Table 4-4 Mesh Convergence Results of Consul.....	36
Table 4-5 Mesh Convergence Results of Jiaolong	36
Table 4-6 The test model characteristics	39
Table 4-7 Verification Results of MT-1 for the FEA Calculation Method	39
Table 4-8 Verification Results of HY-105 for the FEA Calculation Method.....	40
Table 4-9 Verification Results of t0.4-1 for the FEA Calculation Method.....	40
Table 4-10 Analysis Results of Yield Load	41
Table 4-11 Analysis Results of Yield Load (Continued)	42
Table 4-12 Analysis Results of Eigenvalue Buckling	45
Table 4-13 Analyzed Results of Elastic–Plastic Buckling.....	48
Table 4-14 Analyzed Results of Elastic–Plastic Buckling (Continued)	49
Table 4-15 Deviations of Ultimate Strength of FEA for Different Rules.....	49
Table 4-16 Deviations of Ultimate Strength of FEA for Different Rules (Continued) ..	50
Table 4-17 Deviations of Ultimate Strength of FEA for Different Rules (Continued) ..	50
Table 4-18 Deviations of Ultimate Strength of FEA for Different Rules (Continued) ..	50
Table 5-1 Calculated Proposal Thickness Results	56
Table 5-2 Comparison of Ultimate Strength Results.....	56

List of Symbols and Abbreviations

Symbol	Description
DSV	Deep submergence vehicle
AUVs	Autonomous underwater vehicles
ROVs	Remotely operated vehicles
HOVs	Human occupied vehicle
σ_φ	The membrane stress
P	The external pressure
R_m	The mean radius of the spherical pressure shell
σ_y	The yielding strength of the material
t	Thickness of the spherical shell
P_e	The elastic buckling load
E	The elastic modulus of the material (Zoelly)
ν	The Poisson's ratio of the material
P_{es}	The elastic buckling load (Krenzke et al.)
R_o	The outer radius of the spherical pressure shell
P_{cr}	The inelastic buckling load
E_s	The secant modulus of the material
E_t	The tangent modulus of the material
DNVGL	Det Norske Veritas Germanischer Lloyd
DNV	Det Norske Veritas
BV	Bureau Veritas
CCS	China Classification Society
ABS	American Bureau of Shipping
RS	Russian Maritime Register of Shipping
LR	Lloyd's Register rules

Symbol	Description
NK	Nippon Kaiji Kyokai
ψ	The coefficients reflecting post buckling behavior
γ	The load coefficient
γ_m	The material factor
k	The structural slenderness coefficient
Φ	The modification factor
P_e'	The elastic buckling load (BV)
P_f	The modified yield load
η	The modified coefficient (RS)
ΔR	The maximum allowed out-of-circularity
$P_{e''}$	The modified critical elastic buckling load
BSI	British Standards Institution
P_a	The allowable load
K	The coefficients reflecting yield load and buckling load
Δ	The value corresponding the lower bound curve
FEA	Finite element analysis
P_{total}	The evaluation of the buckling load magnitude
P_0	The dead load
P_{ref}	The reference load
λ	The load proportionality factor
R'	The actual measurement radius
\bar{R}	The average radius
Δx	The deviations of the horizontal
Δy	The deviations of the vertical

Chapter 1 Introduction

1.1 Background

1.1.1 Overview of DSV

The ocean covers about 70% of the earth's surface, the average depth of the ocean is about 3.8 km, and the ocean is rich in mineral resources ^[1]. However, for us most of the undersea world remains unknown. Moreover, in recent years, disasters have frequently occurred due to fluctuations in deep sea areas, causing great damage. Needs for various deep-sea exploration such as deep-sea exploration has increased ^[2]. Currently, an increasing number of researchers are keenly interested in the ocean, and various ocean research and energy development are being carried out. Therefore, the demand for deep submergence vehicle (DSV) is increasing as the need for the development, utilization and conservation of marine resources increases ^[3]. With the improvement of ocean exploration and technological advances, the DSV has played a crucial role in underwater survey activities ^[4]. The DSVs are divided into three types: autonomous underwater vehicles (AUVs), remotely operated vehicles (ROVs), and human occupied vehicle (HOVs) ^{[5][6][7]}.

As shown in Figure 1-1, the ROV is connected to the mother ship with a cable, and it can be remotely controlled to observe a specific location in the sea in detail ^[8]. They are common in deep water industries such as oil and gas exploration, telecommunications, geotechnical surveys, and mineral exploration. ROVs may sometimes be referred to as remotely operated underwater vehicles to distinguish them from remotely operated vehicles that operate on land or in the air ^[9]. However, detection, monitoring and video transmission will be an important part of ROVs based applications. In under water, because the distance over which video streams can be transmitted is very limited, wireless communications with higher frequencies cannot work well. ROVs have a limited range of navigation and observation because the range of radio waves that can reach underwater is limited ^[10].

As shown in Figure 1-2, The AUV is an underwater spacecraft that can conduct marine surveys without the need for a mother ship. it has been recognized as a new platform for observing the underwater world. It can dive freely around the mission target specified in the computer before launch ^{[11][12]}. It doesn't need a support device and you can work freely without cables. This has the advantage of low cost without being restricted by the operating range. However, AUVs have energy limitations and have the drawback of not being able to perform complex tasks ^[13].

Introduction

The HOV has the most complex design and manufacturing processes. As shown in Figure 1-3 ^[14]. HOV can carry scientists, engineers and various electronic equipment to quickly and accurately reach various deep-sea complex environments and conduct deep-sea operations. HOV has the advantage that people can go directly into the sea, but the operating cost is high because it is for people to ride, and strict safety measures are required. For this reason, operators are limited to large-scale laboratories and the offshore oil field industry. Division of roles of DSV is shown in Figure 1-4 ^[15].

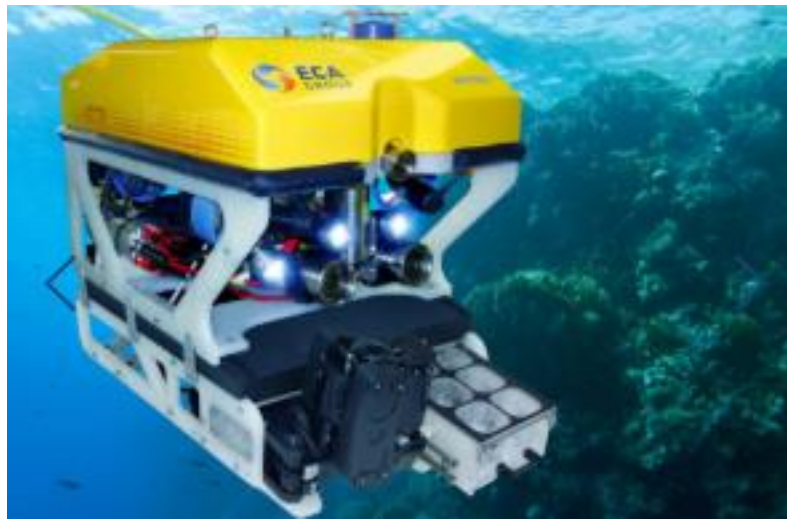


Fig. 1-1 Remotely Operated Vehicle
(Retrieved from <https://www.ecagroup.com>)



Fig. 1-2 Autonomous Underwater Vehicle
(Retrieved from <https://www.meretmarine.com>)



Fig. 1-3 Human Occupied Vehicle
(Retrieved from <https://www.squadron.com>)

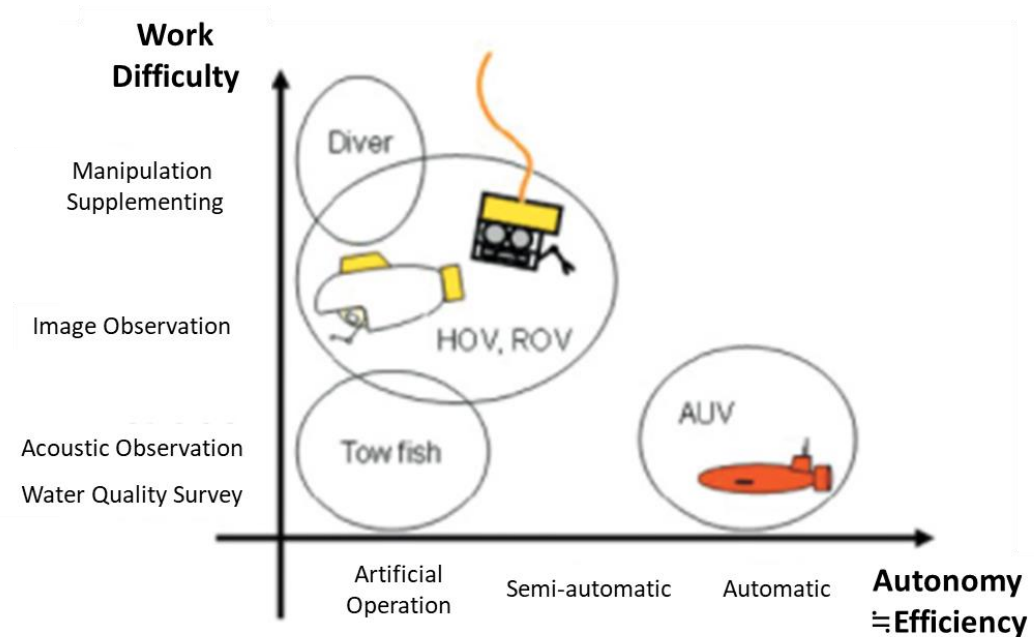


Fig. 1-4 Division of Roles of DSV
(Retrieved from <https://www.jsme.or.jp/kaisi/1199-24/>)

1.1.2 Spherical pressure shells of HOV

Typical HOVs have United States' Alvin, France's Nautil, Russia's Consul, Japan's Shinkai 6500, and China's Jiaolong ^[16]. The pressure shell is the main structure of the HOV, as one of the most critical components and buoyancy units in

the system. It provides safe living space and working space for scientists and investigators. Figure 1-5 is a schematic diagram of spherical pressure shell. The weight of the pressure shell accounts for almost 1/3 of the total weight of a HOV. Therefore, it should be designed to have adequate strength and water tightness ^[17].

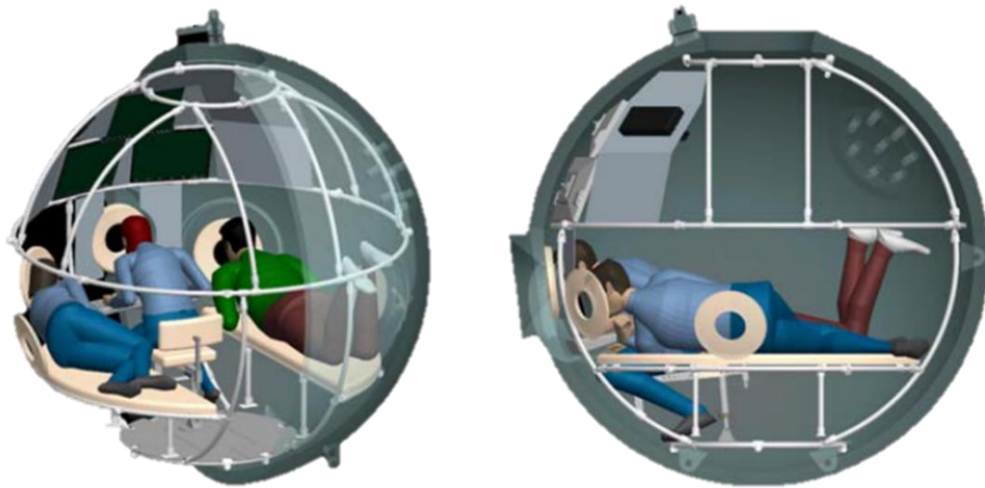


Fig. 1-5 Schematic Diagram of Spherical Pressure Shell

(Retrieved from National Science Foundation <https://www.nsf.gov/>)

Pressure shell is a key component to ensure the safety of submersibles and personnel. The design of pressure shell is directly related to the overall performance and weight index of the submergence vehicle. A reasonable pressure shell can not only meet the requirements of strength and stability, but also ensure that the thickness of the pressure shell is smaller, the structure weight is better, and the material is fully utilized. In order to meet the design requirements, the final supporting strength assessment of the diving preloaded hull is required ^[18]. However, the current design rules for the spherical pressure shells of manned submersibles need to be updated and unified ^{[19][20]}.

Under the premise of ensuring the ultimate strength of the spherical pressure shell, the smaller the mass of the pressure-resistant spherical pressure shell, the more scientific research equipment that the deep submersible can carry, and the greater the underwater function of the deep submersible. Therefore, it is very important to accurately calculate the ultimate strength of the pressure-resistant spherical shell. For the ultimate strength of the spherical shell structure, many scholars have conducted research on it and conducted corresponding experiments. In 2014, Vedachalam, et al. based on applicable standards, reliability analysis is done on 5

key representative functions with the assumption that the submersible is utilized for ten deep water missions per year ^[21]. A typical pressure shell is a closed medium-thickness revolving hull under uniform external pressure, which is prone to nonlinear buckling. The buckling characteristics are greatly affected by geometric configuration, wall thickness, material properties and inevitable initial geometric defects ^{[22][23]}. Blachut found that both geometrical imperfections and material plasticity could lead to a severe decrease in the load carrying capacity of shells ^{[24][25][26]}.

As this involves direct human presence, the system and structure have to be extremely reliable. Lu et al. ^[27] used nonlinear finite elements to calculate the ultimate strength of a series of radius-thickness ratios and different initial perturbations of pressure-resistant spherical pressure shells and carried out several major calculation formulas for the ultimate strength of spherical shells for comparison.

Cho et al. ^[28] considered the influence of transverse shear deformation on the ultimate strength of the pressure-resistant spherical pressure shell on the basis of predecessors. Wunderlich et al. ^[29] discussed the influence of the openings on the spherical pressure shell, the initial imperfections and the local initial disturbance on the ultimate strength of the spherical pressure shell. The eigenvalue buckling mode is obtained to deal with the initial disturbance, which is the most unfavorable form of the structure.

In summing up the work of predecessors, combined with the existing calculation formula of the ultimate strength of the spherical shell, a series of pressure-resistant spherical shell model tests were carried out, and an empirical formula for calculating the ultimate strength was given. Liu et al. ^[30] took the spherical pressure shell with a reinforced structure with openings as the research object, and conducted a finite element analysis on the sample points of the reinforced structure with openings, and a more robust design flow is obtained.

1.2 Motivation and innovations

According to above literature review, the strength of the spherical pressure shell of a human occupied vehicle is important. A reasonable pressure shell can not only meet the requirements of strength and stability, but also ensure that the thickness of the pressure shell is smaller, the structure weight is better, and the material is fully utilized. In order to meet the design requirements, the final supporting strength

Introduction

assessment of the diving preloaded hull is required.

Nowadays, each classification rule provides an evaluation method for the ultimate strength of the spherical pressure shell to ensure that structural scantling can meet the requirements. However, in fact, the design methods of classification rules have not been discussed and unified.

According to the design results of this research, there are significant differences in the design results of various classification rules. However, the validity of the design results also cannot be easily confirmed without numerical analyses and model experiments.

Therefore, the main purpose of this research mainly focuses on the design results obtained based on the various classification rules and proposes a design method to estimate the scantling of spherical pressure shells. Since the actual pressure shells are assembled by bending and welding, it is inevitable that initial imperfections and residual stresses will inevitably occur during the production process, and the actual strength of pressure shells will be reduced from the theoretical value. The design method proposed by this research institute also discussed this initial imperfection and brought the design results closer to the actual situation. This method can reduce the waste of design time and reduce estimation errors.

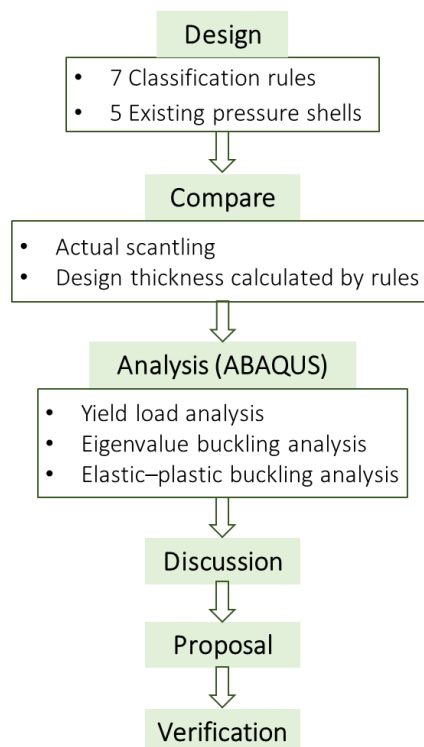


Fig. 1-6 Research Map of the Thesis

1.3 Structure of the thesis

This thesis is composed of 6 chapters. The structure of this thesis is as follows:

Chapter 1: Introduction

This chapter will briefly introduce some background information of the spherical pressure shell and explain the research status and existing problems. Finally, the research purpose of this thesis is described.

Chapter 2: Criteria and formulas

Describes the theoretical formula of ultimate strength for spherical pressure shell. The design formulas of various classification associations and other standards are also introduced in this chapter.

Chapter 3: Design of spherical pressure shells

To unify the design method of the pressure shell and confirm its accuracy, this research herein recalculated the thickness of five existing spherical pressure shells using the different classification rules and discuss them.

Chapter 4: Structural analysis

Presents three kinds of analysis were conducted in ABAQUS for this research: yield load analysis, eigenvalue buckling analysis and elastic-plastic buckling analysis (ABAQUS / Riks method). Discuss the analyzed results of the stress and stability for spherical pressure shells subjected to external pressure. The effectiveness of the analysis method of this research are also identified in this chapter.

Chapter 5: Proposal

This thesis proposes a design method that estimated the scantling of the spherical pressure shell and conducted simulations to verify the accuracy of the proposed design method.

Chapter 6: Conclusions and future work

Summarizes the conclusions of the above chapters and recommendations future works.

References

- [1] V. Faraoni: Exercises in Environmental Physics. New York, Springer Science & Business Media, 2006.
- [2] N. A. Raineault, K. L. C. Bell, and P. Girguis: Advancing Ocean Science and Exploration Through Telepresence, Deep Sea Research Part II: Topical Studies in Oceanography, vol. 150, pp. 1-3, April 2018.
- [3] 藤岡換太郎: 深海から地球を考える, 建設コンサルタンツ協会誌, vol. 251, 2011.
- [4] L. Whitcomb, D. R. Yoerger, H. Singh, and J. Howland: Advances in Underwater Robot Vehicles for Deep Ocean Exploration: Navigation, Control, and Survey Operations, Robotics Research, London, Springer, 2000.
- [5] S. E. Humphris and A. Soule: Vehicles for Deep-Sea Exploration, Encyclopedia of Ocean Sciences (Third Edition), vol. 5, pp. 21-30, 2019.
- [6] 文部科学省, 今後の深海探査システムの在り方について, 科学技術・学術審議会海洋開発分科会第4回会合, 2016.
- [7] Y. Wu, X. Ta, R. Xiao, Y. Wei, D. An, and D. Li: Survey of Underwater Robot Positioning Navigation, Applied Ocean Research, vol. 90, 2019.
- [8] Remotely Operated Underwater Vehicle: Retrieved from <https://ja.wikipedia.org/wiki/ROV>.
- [9] 上村宇之, 増田慎哉: 水中ロボットの産業活用 - 水中ロボットの産業活用の実例と歴史, マリンエンジニアリング, vol. 54, no. 6, pp. 844-847, 2019.
- [10] F.A. Azis, M.S.M. Aras, M.Z.A. Rashid, M.N. Othman, and S.S. Abdullah: Problem Identification for Underwater Remotely Operated Vehicle (ROV): A Case Study, Procedia Engineering, vol. 41, pp. 554-560, 2012.
- [11] 浦環, 自律型海中ロボットの発展する方向, 地学雑誌, vol. 109, no. 6, pp.900-906, 2000.
- [12] A. Sahoo, S. K. Dwivedy, and P.S. Robi: Advancements in the Field of Autonomous Underwater Vehicle, Ocean Engineering, vol. 181, no. 1, pp. 145-160, June 2019.
- [13] 吉田弘, 百留忠洋, 石橋正二郎, 澤隆雄, 志村拓也: 深海自律形無人探査機とその要素技術の最前線—通信衛星による海洋ネットワークの話題等—, 電子情報通信学会通信ソサイエティマガジン, vol. 5, no. 2, pp. 127-136, 2011.
- [14] W. Cui, S. Fu and Z. Hu: Human Occupied Vehicle (HOV), Encyclopedia of Ocean Engineering, Singapore, Springer, pp. 1-8, 2018.

- [15] 卷俊宏, AUV : 自律型海中ロボット, 日本機械学会誌, vol. 121, 2018.
- [16] W. Kohnen: Review of Deep Ocean Manned Submersible Activity in 2013. Marine Technology Society Journal, vol. 47, pp. 56-68, 2013.
- [17] J. Blachut and P. Smith: Buckling of Multisegment Underwater Pressure Hull, Ocean Engineering, vol. 35, pp. 247-260, 2008.
- [18] S. Yuan, Q. Chen, and K. Ye: Simulation and Evaluation of Ultimate Strength Based Safety Factor for Titanium Alloy Spherical Pressure Hull, MARSTRUCT 2019, International Conference on Marine Structures, Dubrovnik, Croatia, 2019.
- [19] Y. Huang, K. Minami, and M. Masuda: A proposed design method for spherical pressure shell under external pressure, Asia Navigation Conference (ANC - 2019), Busan, Korea, November 2019.
- [20] B. B. Pan, W. C. Cui, Y. S. Shen, and T. Liu: Further study on the ultimate strength analysis of spherical pressure hulls, Marine Structures, vol. 23, pp. 444-461, 2010.
- [21] G. Luo, Y. Huang, C. Liang, and C. Hsu: The influence of frame proportions on buckling strength of a pressure hull, Journal of Taiwan Society of Naval Architects and Marine Engineers, vol. 35, no. 3, pp. 123-133, 2016.
- [22] G. Luo and Y. Huang: Non-linear buckle analysis of stiffened cylindrical pressure hull, The 4th Annual conference on Engineering and Information Technology (ACEAIT-2016), Kyoto, Japan, March 2016.
- [23] N. Vedachalam, G. A. Ramadass, and M. A. Atmanand: Reliability Centered Modeling for Development of Deep Water Human Occupied Vehicles, Applied Ocean Research, vol. 46, pp. 131-143, June 2014.
- [24] J. Blachut: Buckling of Externally Pressurized Steel Toriconical Shells, International Journal of Pressure Vessels and Piping, vol. 144, pp. 25-34, August 2016.
- [25] J. Blachut: Locally Flattened or Dented Domes Under External Pressure, Thin-Walled Structures, Vol. 97, pp. 44-52, December 2015.
- [26] J. Blachut: Buckling of Multilayered Metal Domes, Thin-Walled Structures, vol. 47, no. 12, pp. 1429-1438, December 2009.
- [27] B. Lu, T. Liu, and W. Cui: Ultimate Strength of Pressure Spherical Hull in Deep-sea Manned Submersibles, Journal of Ship Mechanics, vol. 11, no. 2, pp. 214-220.
- [28] S. Cho, Q. Do, and H. Shin: Residual Strength of Damaged Ring-Stiffened Cylinders Subjected to External Hydrostatic Pressure, Marine Structures, vol. 56, pp. 186-205, August 2017.
- [29] W. Wunderlich and U. Albertin: Buckling Behaviour of Imperfect Spherical

- Shells, *International Journal of Non-Linear Mechanics*, vol. 37, pp. 589-604, 2002.
- [30] F. Liu, D. Han, and J. Yao: Robust Optimization of a Pressure Spherical Shell With a Strengthened Opening, *Journal of Harbin Engineering University*, vol. 37, no. 12, pp. 1613-1637, 2016.

Chapter 2 Criteria and formulas

2.1 Introduction

The ultimate strength of spherical pressure shells has been the subject of the numerous design attempts. There are two possible spherical pressure-shell failure modes after they are subjected to the ultimate pressure, whereby the maximum stress of the spherical shell reaches the yield strength of the material and leads to the collapse of the elastic or plastic ranges. The former modes refer to stress analysis, whereas the latter refer to stability analysis. When a spherical pressure shell is imposed to a uniform external pressure, the membrane stress σ_ϕ in the spherical pressure shell can be calculated by Equation 2-1.

$$\sigma_\phi = \frac{PR_m}{2t} \quad (2-1)$$

When the membrane stress in the spherical shell reaches the yield point of the material, it is regarded to be the maximum allowable stress. The yield point is the first stress in the material, which is less than the maximum available stress. At this time, the strain increases but the stress does not increase. The yield point can be determined by stopping the pointer or by self-drawing. A total elongation of 0.5% under load is also considered acceptable. Accordingly, the yield load P_y can be calculated by Equation 2-2, whereby P is the external pressure, R_m is the mean radius of the spherical pressure shell, σ_y is the yielding strength of the material, and t is the thickness of the spherical shell.

$$P_y = \frac{2\sigma_y t}{R_m} \quad (2-2)$$

The classical elastic buckling theory used to calculate the ultimate strength of the complete spherical shells subjected to external pressure was first derived by Zoelly in 1915^[1]. Zoelly utilized the classical theory of small deflections and assumed that the spherical shell geometry is perfect with isotropic material properties. Based on the aforementioned methods, a formula was proposed for the elastic buckling load

of the spherical shell based on which the elastic buckling load P_e can be calculated by Equation 2-3. E denotes the elastic modulus of the material and ν is the Poisson's ratio of the material.

$$P_e = \frac{2E}{\sqrt{3(1-\nu^2)}} \left(\frac{t}{R_m} \right)^2 \quad (2-3)$$

However, everyone will recognize that the actual manufacturing process is almost impossible to maintain perfect geometric shapes. Due to geometric defects and material properties, the evaluation was found to be much higher than the experimental results. Therefore, the elastic buckling theory proposed by Zoelly was established only for perfect spherical shell states and is not suitable for the calculation of the ultimate strengths in the cases of actual pressure shells.

In the tests reported by Krenzke and Kiernan in 1963 based on the David Taylor Model Basin ^[2], the actual buckling load was proposed to be approximately equal to 0.7 times the value of the elastic buckling load. The experimental results were based on a series of tests of more than 200 small spherical shell models with varying degrees of initial imperfections. The formula of elastic buckling load P_{es} derived by Krenzke et al. is expressed by Equation 2-4, whereby R_o is the outer radius of the spherical pressure shell.

$$P_{es} = \frac{1.4E}{\sqrt{3(1-\nu^2)}} \left(\frac{t}{R_o} \right)^2 \quad (2-4)$$

By considering the inelastic stress-strain performance, the secant and tangent moduli could replace the elastic modulus. Thus, the formula of the inelastic buckling load P_{cr} can be expressed according to Equation 2-5. The spherical pressure shell of Shinkai 6500 is also designed based on these two formulas, whereby E_s and E_t are the secant and tangent modulus of the material, respectively.

$$P_{cr} = 1.4 \sqrt{\frac{E_t \cdot E_s}{3(1-\nu^2)}} \left(\frac{t}{R_o} \right)^2 \quad (2-5)$$

2.2 Estimation method of classification society

Nowadays, each classification society has its own evaluation criteria for determining the minimum scantling requirements of spherical pressure shells. These include the Det Norske Veritas Germanischer Lloyd, Det Norske Veritas, Bureau Veritas, China Classification Society, American Bureau of Shipping, Russian Maritime Register of Shipping, and Lloyd's Register rules. Moreover, among all the rules, only ABS and RS rules clearly stipulates that its formula can be used for the calculation of titanium structures; other rules should only be applied to steel structures, and titanium structures should be considered as a special case.

In this section, the design formulas and requirements of various classification associations for spherical pressure shell structures will be introduced in detail. For clarity and simplicity, the names of the classification rules are represented by abbreviation as follows: Det Norske Veritas Germanischer Lloyd (DNVGL), Det Norske Veritas (DNV), Bureau Veritas (BV), China Classification Society (CCS), American Bureau of Shipping (ABS), Russian Maritime Register of Shipping (RS), Lloyd's Register rules (LR), and Nippon Kaiji Kyokai (NK).

2.2.1 DNVGL

The DNV GL classification rules contain procedures and technical requirements related to obtaining and retaining a classification certificate. These rules represent all the requirements adopted by the Society as the basis for classification. Failures that are critical to stability and plastic failure should be analyzed. The structural load caused by the weight of the pressure shells or any fastening components should not cause any excessive stress increase on the pressure shell surface. The pressure shell wall of the load bearing or lead-in area, such as the area of welded supports and brackets, should be reinforced accordingly. If used, the corners of the reinforcing plate must be rounded sufficiently to avoid increasing welding stress. Exceptions must be agreed with DNV GL.

The reduction in elastic modulus between the proportional limit and the defined yield point or 0.2% plastic strain limit, respectively, should be considered. Generally, the material should be assumed to be elastic and plastic, and strain hardening should not be considered. As mentioned in the introduction, all current design rules are based on the classic yield load formula and the theoretical elastic buckling formula, but there are subtle differences between different rules. DNVGL rules^[3] are based on these two formulae for pressure shell strength evaluation of a pressure shell. The

yield load P_y is calculated with Equation 2-2 and the elastic buckling load P_{es} of the spherical shell is calculated with Equation 2-4.

2.2.2 Det Norske Veritas (DNV)

DNV has been merged with GL in 2013, the new DNV GL rules of spherical pressure shell is different from the original DNV rules. In this research we refer to the DNV rule chapter D100 "Structural analysis", which was published in 1988 [4]. A complete structural analysis based on recognized methods may be accepted, or it may be required as the basis for determining the internal or external pressure dimensions of the pressure vessel. Analysis tools can be finite element analysis and shell theory. Analysis tools and models will be documented. The design stress shall comply with the recognized norms accepted by the DNV Association.

The DNV rules are mainly based on the classic yield load formula for strength evaluation, and the strength loss caused by structural imperfections is also considered. The primary design equations of spherical pressure shells are calculated with Equation 2-6 and Equation 2-7.

Whereby ψ is coefficients reflecting post buckling behavior can be obtained from Table 2-1, γ is load coefficient can be determined by Table 2-2.

$$P \leq P_a = \frac{P_z \cdot \psi}{\gamma \cdot \gamma_m \cdot k} \quad (2-6)$$

Table 2-1 Coefficient of Reflecting Post Buckling Behavior (ψ)

Types of Pressure Shells	ψ
Cylinders, Cones	0,9
Spheres, Hemispheres, Torispheres and Ellipsoides	0.75

γ_m is the material factor. k is the structural slenderness coefficient, this coefficient depending on type of structural member under consideration, it can be obtained from Table 2-3.

Φ is the modification factor which reflects the slenderness and structural imperfections.

$$P_{cr} = 2 \cdot \Phi \frac{t}{R_m} \sigma_y \quad (2-7)$$

Table 2-2 Load Coefficient (γ)

P (bar)	$P \leq 20$	$20 < P < 50$	$P \geq 50$
γ	1.3	$0.33(4.3 - 0.02P)$	1.1

Table 2-3 S Coefficient of Structural Slenderness (k)

Slenderness ratio λ	$\lambda < 0.5$	$0.5 \leq \lambda \leq 1$	$1 < \lambda$
k	1	$0.7 + 0.6\lambda$	1.3

All these coefficients can be regarded as additional factors representing the uncertainty of the structure and materials. In addition to looking up the table, these coefficients can also be calculated by Equation 2-8 to Equation 2-11.

$$\Phi = \frac{1}{\sqrt{1 + \lambda^4}} \quad (2-8)$$

$$\lambda = \sqrt{\frac{\sigma_y}{\sigma_e}} \quad (2-9)$$

$$\sigma_e = 0.605 \rho \frac{t}{R_m} E \quad (2-10)$$

$$\rho = \frac{0.5}{\sqrt{1 + \frac{R_m}{100 \cdot t}}} \quad (2-11)$$

2.2.3 American Bureau of Shipping (ABS)

In this research, we refer to Chapter 23 "Spherical Shells Under External Pressure" of the ABS rules, the metal pressure boundary of pressure shells and manned pressure vessels should be designed according to all expected pressures and loads that may act on the pressure boundary under normal and emergency operating conditions.

ABS rules ^[5] divide the design method based on two collapse problems. In the first stage, when t/R is small, the critical elastic buckling load P_e of the shell is less than or equal to the yield load P_y , the pressure shell mainly collapses due to buckling. Generally thin spherical shells belong to the first stage, as shown in Equation 2-12.

$$P_{cs} = 0.2124P_e \quad \text{for} \quad \frac{P_e}{P_y} \leq 1 \quad (2-12)$$

In the second stage, as t/R increases, the pressure shell mainly collapses due to yielding, which means that the stresses in the spherical shell reach the yield strength of the material, as shown in Equation 2-13.

$$P_{cs} = P_y \cdot 0.7391 \left[1 + \left(\frac{P_y}{0.3P_e} \right)^2 \right]^{-\frac{1}{2}} \quad \text{for} \quad \frac{P_e}{P_y} > 1 \quad (2-13)$$

2.2.4 Lloyd's Register of Shipping (LR)

In the LR rules ^[6], material coefficients are considered when evaluating structural stability. The elastic buckling load P_{es} of the spherical shell is calculated with Equation 2-3 and the modified yield load P_{ys} can be calculated by Equation 2-14, where sf is safety factor.

$$P_{ys} = \frac{\gamma_m}{sf} P_y \quad (2-14)$$

2.2.5 Bureau Veritas (BV)

According to the BV rules ^[7], The design of the diving system and its components should meet the conditions for which it is permitted to operate. In particular, the design pressure of the pressure vessel as a part of the life support system should be at least equal to the maximum working depth.

In the BV rules, the safety factor is considered in the calculation of the yield load, and regards the safety factor as a structural imperfection, and provides a design curve as shown in Figure 2-1. w is defined as structural imperfection factor. The structural imperfection factor is considered in the calculation of the elastic buckling load. P_e' is

the failure pressure due to elastic instability, as given in Equation 2-15, it can be regarded as a modified elastic buckling load.

$$P_e = \frac{9.6E}{9 + 0.003\left(\frac{2R_o}{t}\right)} \left(\frac{t}{2R_o}\right) \quad (2-15)$$

P_f can be regarded as a modified yield load, as shown in Figure 2-2. When evaluating the ultimate strength when the structure is failure, the minimum value of the modified buckling load and the modified yield load shall be taken as a conservative design, as show in Equation 2-16.

$$P_u = \min(P_e, P_f) \quad (2-16)$$

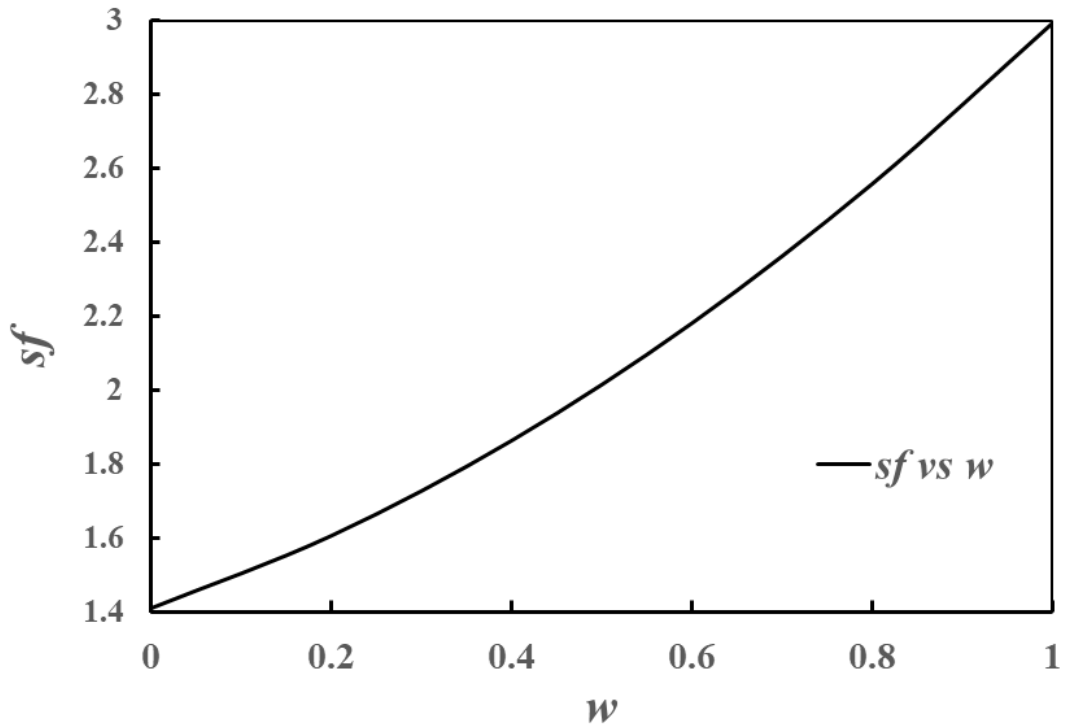


Fig. 2-1 Structural Imperfection Factor ^[7]

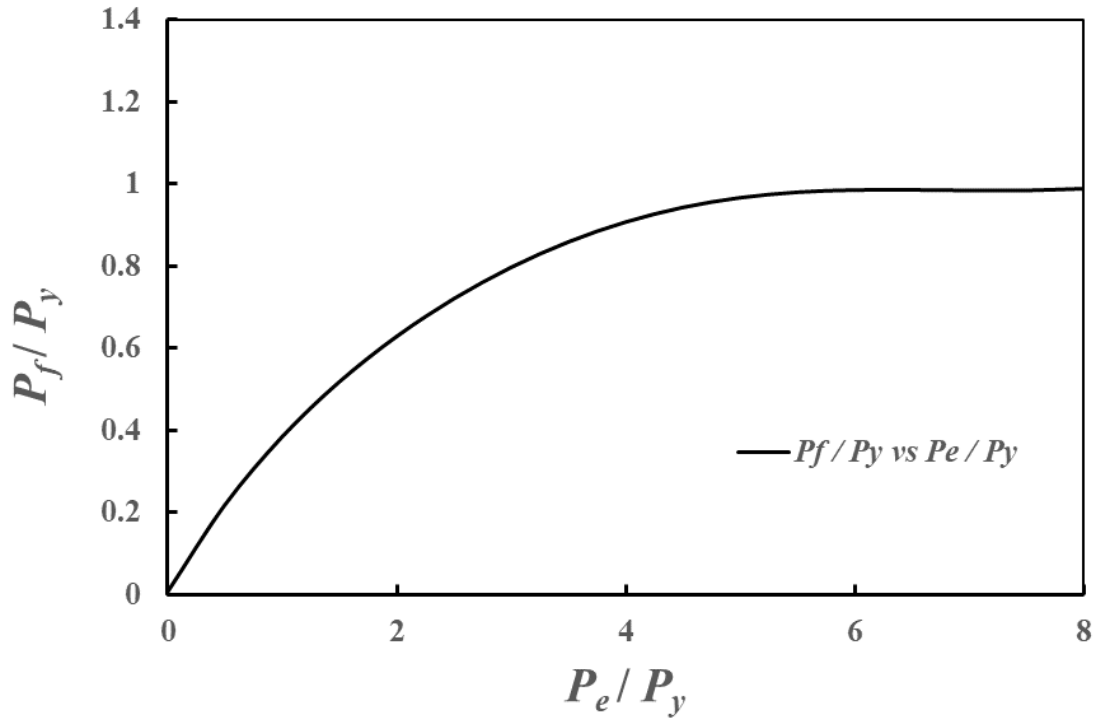


Fig. 2-2 Correction Curve of Elastic Buckling Load ^[7]

2.2.6 Russian Maritime Register of Shipping (RS)

Here, this research refer to Section 3 "Classification surveys of manned submersibles and ships diving systems under construction" in the RS rules issued in 2018. The requirements of this section apply to the pressure structures of manned submersibles, ship diving systems and manned submersibles. The basic formula given below can evaluate the strength, and can also check the stability of stiffened and unstiffened cylindrical and conical shells, as well as spherical shells and tanks, hemispherical and nearly hemispherical ends. Considering that the thickness of structural members should be calculated, in most cases, several formulas should be used to calculate the strength as a check calculation for the selected dimensions of hull structural members.

The calculation equation of RS rules ^[8] is based on the Equation 2-17 and Equation 2-18, and these two equations need to be established at the same time. Equation 2-17 is to confirm the failure caused by the membrane stress, Equation 2-18 it is to confirm that the pressure at the time of buckling failure has exceeded the design pressure.

$$\sigma_{\phi} \leq \sigma_y \quad (2-17)$$

$$P_a = \frac{\eta P_e}{sf} \geq P \quad (2-18)$$

where, η is the modified coefficient due to the non-linear characteristics of the material and structural imperfections, as shown in Equation 2-19 to Equation 2-21.

In Equation 2-22, ΔR is the maximum allowed out-of-circularity.

$$\eta = \frac{\eta_s}{\sqrt{1 + [\eta_s \delta (1 + f_s)]^2}} \quad (2-19)$$

$$\eta_s = \frac{1}{1 + (2.8 + f_s) f_s^{\frac{2}{3}}} \quad (2-20)$$

$$\bar{\delta} = \frac{P_e R}{2 \cdot t \cdot \sigma_y} = \frac{P_e}{P_y} \quad (2-21)$$

$$f_s = \frac{\Delta R}{t} \quad (2-22)$$

2.2.7 China Classification Society (CCS)

In this section, we introduce the pressure shell design in the CCS rules published in 2018 ^[9]. According to the Chapter 4 "Design of pressure hulls" of the CCS Rules, it is applicable to steel pressure shells, including the design of reinforced structures. The design methods and strength criteria specified in this chapter shall be based on the premise that the manufacturing tolerances meet the manufacturing requirements. When the tolerance limit is exceeded, appropriate strengthening measures should be

taken, otherwise the maximum working pressure needs to be reduced accordingly. The internal pressure and external pressure shell shall be calculated and checked in accordance with the requirements of this chapter in accordance with the operational requirements for the pressure shell to withstand internal pressure and external pressure, and shall comply with the corresponding regulations.

The design method of the CCS rules is similar to that of the BV rules and RS rules. The yield load and elastic buckling load are considered during the design process, and the minimum value of these loads is used as the ultimate strength. On the other hand, it is also necessary to consider whether the membrane stress and buckling load meet the design requirements. The calculation equation is separated into two parts. The first part is failure due to membrane yield, as shown in Equation 2-23, the membrane stress should be less than 85% of the material yielding strength.

$$\sigma_{\phi} \leq 0.85 \sigma_y \quad (2-23)$$

The second part is failure due to buckling, as shown in Equation 2-24. Whereby $P_{e''}$ can be treated as the modified critical elastic buckling load as shown in Equation 2-25. The coefficient C can be obtained from Figure 2-3.

$$P \leq \Delta R \cdot \gamma_m \cdot P_{e''} \quad (2-24)$$

$$P_{e''} = 0.84 E C^2 \quad (2-25)$$

2.2.8 Nippon Kaiji Kyokai (NK)

The part T "Construction and Strength of Pressure Hulls and Pressure Enclosures" in NK rules published in 2018, the construction and strength considered appropriate are those to comply with the requirements design pressure and design temperature. The design pressure is to be a pressure corresponding to the design diving depth or more. For submersibles operated in designated service areas, the design temperature is not to be less than 25°C.

There are no detailed design formulas in the Nippon Kaiji Kyokai rules ^[10]. However, they set the criteria for the safety strength such that the ultimate strength

of the pressure shell is capable of withstanding 150% of the developed pressure at the operating depth plus the hydrostatic pressure at the depth of 300 m. The design pressure of the Shinkai 6500 pressure shell was set according to this requirement, with the use of the safety factor of 1.55 ^[11].

2.3 BSI specification PD 5500

PD 5500 ^[12] is the specification for unfired fusion welded pressure vessels, it is a design code set by the British Standards Institution (BSI) for pressure vessels. It can perfectly design pressure shell of different shapes for both external pressure and internal pressure.

The experimental curve is usually used in the pressure shell design. The BSI specification provides a lower bound curve for the pressure shell design. This lower bound curve represents the data obtained from the actual test comprising 700 pressure shells. In addition, titanium and titanium alloy structures are also allowed. Moreover, various levels of safety factors are considered. The lower bound curve of the BSI specification is shown in Figure 14. Generally, the K value can be obtained after the yield load and the buckling load have been calculated using the formula. The corresponding Δ value can be determined using the lower bound curve, and the allowable load P_a , which is the ultimate strength of the design, can be calculated.

According to the BSI specification, the convenient approximation of P_a which is within 1% of the lower bound curve can be obtain with Equation 2-26 and 2-27. It can be known that if yield will occur before buckling, P_a can be obtained by the Equation 2-26. On the contrary, the buckling load is less than the yield load, P_a can be obtained by the Equation 2-27, in this case, P_a is approximately $P_e/2$.

$$\frac{P_e}{p_y} \geq 1 \quad , \quad P_a \cdot sf = p_y - \frac{P_y^2}{2P_e} \quad (2-26)$$

$$\frac{P_e}{p_y} < 1 \quad , \quad P_a \cdot sf = \frac{P_e}{2} \quad (2-27)$$

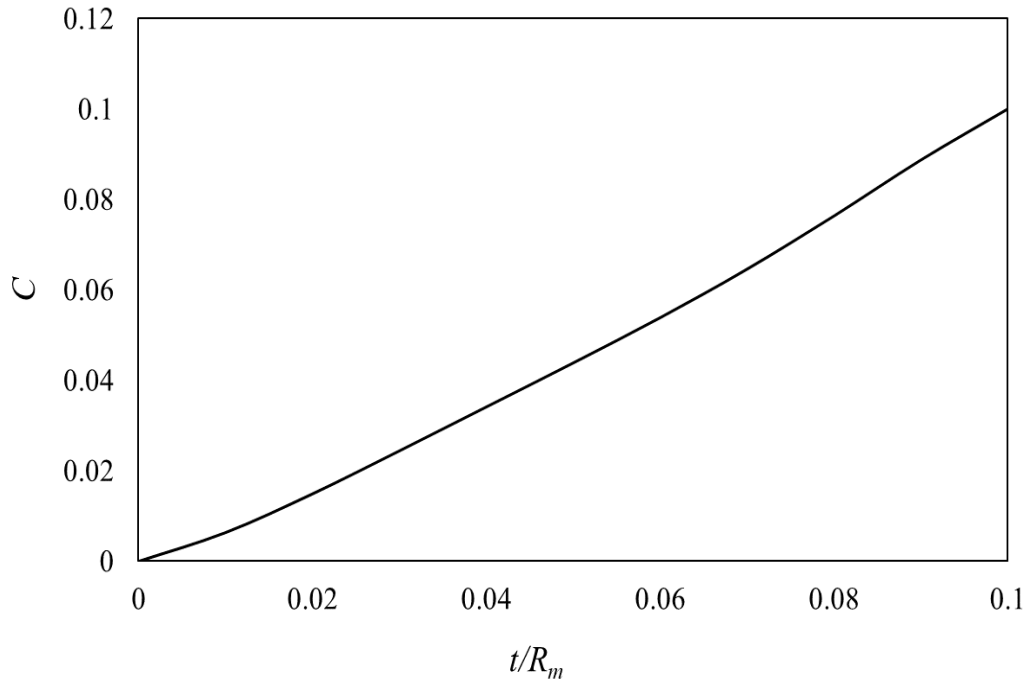


Fig. 2-3 The coefficient C versus t/R_m ^[9]

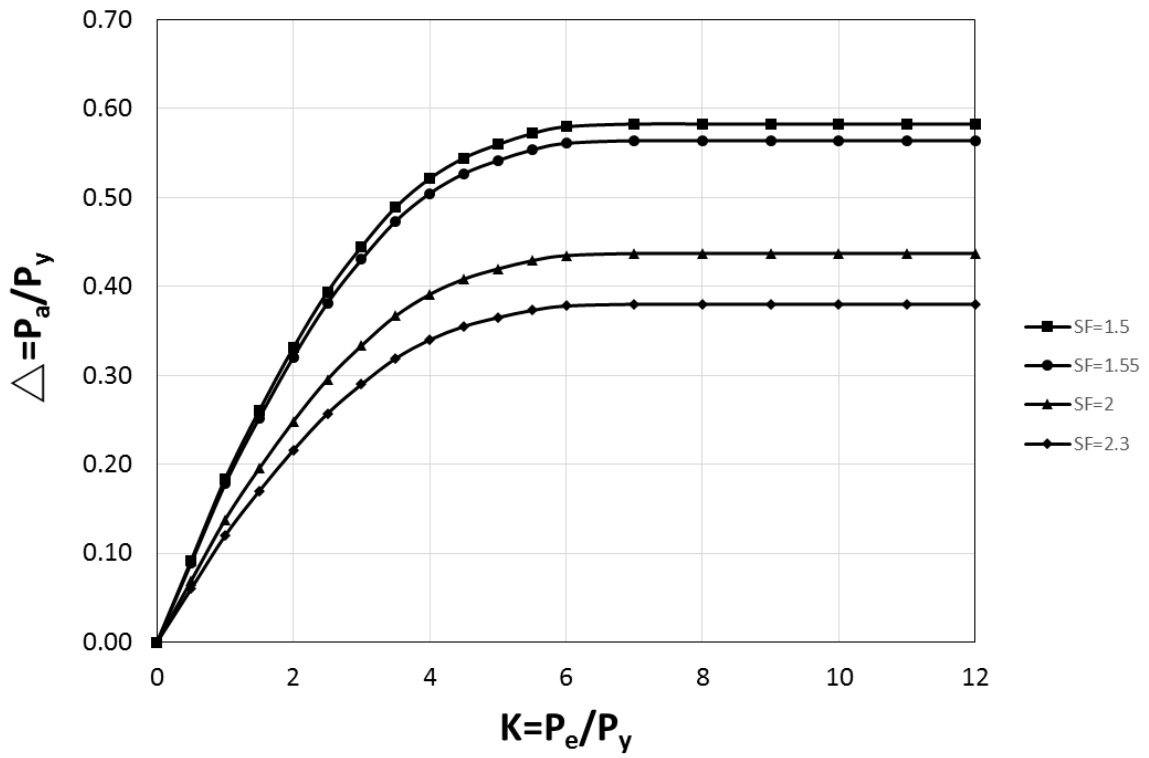


Fig. 2-4 Lower bound curve of the PD 5500 ^[12]

References

- [1] Robert Zoelly: Über ein Knickungsproblem an der Kugelschale, Ph.D. Dissertation, Eidgenössische Technische Hochschule, Zurich, Switzerland, 1915.
- [2] M. A. Krenzke and T. J. Kiernan: Test of Stiffened and Unstiffened Machined Spherical Shells Under External Hydrostatic Pressure, Mechanics Laboratory Research and Development Report, David Taylor Model Basin, August 1963.
- [3] Det Norske Veritas Germanischer Lloyd: Rules for Classification Underwater Technology, DNV GL, 2018.
- [4] Det Norske Veritas: Rules for Certification of Diving System, DNV, 1988.
- [5] American Bureau of Shipping: Rules for Building and Classing Underwater Vehicles, Systems, and Hyperbaric Facilities, ABS, 2019.
- [6] Lloyd's Register: Rules and Regulations for the Construction and Classification of Submersibles and Diving Systems, LR, 2019.
- [7] Bureau Veritas: Rules for the Classification of Naval Submarines, BV, 2016.
- [8] Russian Maritime Register of Shipping: Rules for the Classification and Construction of Manned Submersibles and Ship's Diving Systems, RS, 2018.
- [9] China Classification Society: Rules for Classification of Diving Systems and Submersibles, CCS, 2018.
- [10] Nippon Kaiji Kyokai: Rules for the Survey and Construction of Steel Ships, NK, 2018.
- [11] S. Takagawa, D. Kiuchi, K. Takahashi, Y. Yamauchi, K. Inoue, and T. Nishimura: Design and Construction of Spherical Pressure Hull of SHINKAI 6500, Report of Japan Marine Science and Technology Center (JAMSTEC), Rep. 23, pp. 329–343 March 1990.
- [12] British Standards Institution: Specification for Unfired Fusion Welded Pressure Vessels, BSI, 2016.

Chapter 3 Design of spherical pressure shells

3.1 Introduction

Although all classification rules are related to the classical yield load formula and elastic buckling load formulas used for estimating the ultimate strength, the design coefficients, estimation methods, and evaluation criteria of various classification rules are not the same. Consequently, the corresponding calculated results will be different. To unify the design method of the pressure shell and confirm its accuracy, we herein recalculated the thickness of five existing spherical pressure shells using the different classification rules introduced in Chapter 2.

NK rules do not list detailed formulas on how to determine the ultimate strength of the spherical pressure shell. Therefore, this research did not use the NK rules as a comparison target.

3.2 Design objects and material properties

Herein, the design objects of spherical pressure shells are the United States' Alvin, France's Nautilus, Russia's Consul, Japan's Shinkai 6500, and China's Jiaolong^{[1][2][3][4]}. Table 3-1 lists the characteristics and design conditions of the five existing pressure shells.

The five pressure shells studied and compared herein were all fabricated using titanium alloy. Shinkai 6500 uses Ti-6Al-4V ELI; Alvin uses Ti6211; and the other pressure shells use Ti-6Al-4V. As shown in Table 3-2. The material properties are shown in Table 3-3. The stress–strain curve of Ti-6Al-4V is shown in Figure 3-1^[5].

Table 3-1 Characteristics of the Existing Human Occupied Vehicles (HOVs)

Name	Operating Depth (m)	Internal Diameter D_i (mm)	Safety Factor sf	Actual Thickness t_{ac} (mm)
Shinkai 6500	6500	2000	1.55	73.5
Alvin	4500	2000	1.5	51
Nautilus	6000	2100	1.5	62
Consul	6000	2100	1.5	71
Jiaolong	7000	2100	1.5	77

Table 3-2 Material of the Existing Human Occupied Vehicles (HOVs)

Name	Shinkai 6500	Alvin	Nautile	Consul	Jiaolong
Material	Ti-6Al-4VELI	Ti6211	Ti-6Al-4V	Ti-6Al-4V	Ti-6Al-4V

Table 3-3 Material Properties

	Ti-6Al-4V	Ti-6Al-4V ELI	Ti-6211
Elastic Modulus E (MPa)	114800	113800	115000
Yield Strength (0.2% offset) σ_y (MPa)	872	790	790
Poisson's Ratio ν	0.33	0.342	0.31
Density ρ (kg/m ³)	4423	4430	4480

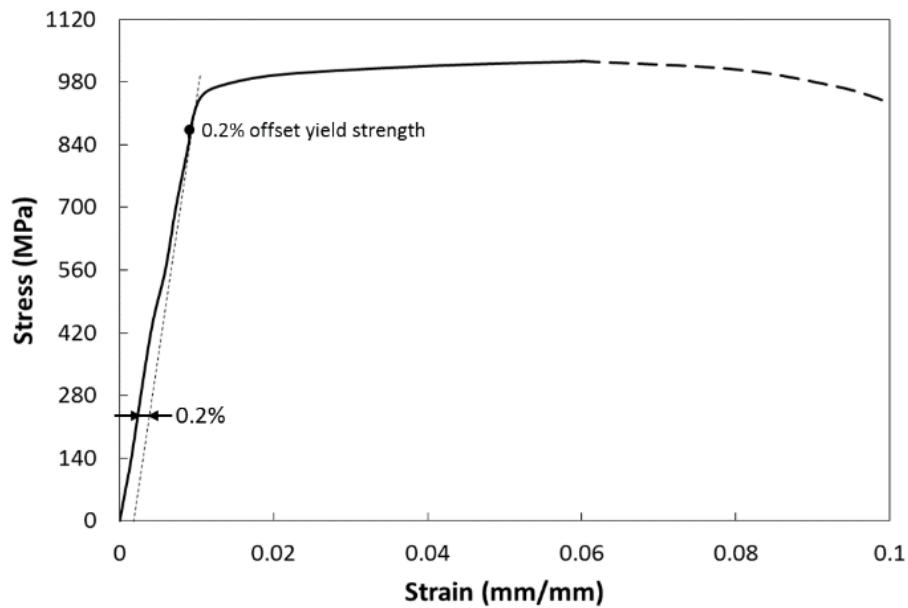


Fig. 3-1 Stress–Strain Curve of Ti-6Al-4V

3.3 Comparison of classification rules

The thickness of five existing spherical pressure shells was recalculated using different classification rules. The calculation results are shown in Table 3-4 to Table 3-7.

Design of spherical pressure shells

According to the comparison results listed in Table 3-4 to Table 3-7, it can be found that the actual thickness of a pressure shell has a tendency to be considerably smaller than the design thickness calculated based on classification rules. Conversely, this research found out that the deviation of the design results between BV and ABS is too conservative. The design thickness is approximately 20% to 30% larger than the actually used thickness. It can be observed that many existing pressure shells are not in compliance with most classification rules.

Table 3-4 Comparison of Actual Thickness and Design Thickness

Ref. HOV	RS		DNV	
	t (mm)	Deviation (%)	t (mm)	Deviation (%)
Shinkai 6500	73.00	0.68	76.20	-3.54
Alvin	51.20	-0.39	57.20	-10.84
Nautile	63.70	-2.67	70.90	-12.55
Consul	63.70	11.46	70.90	0.14
Jiaolong	73.10	5.34	80.10	-3.87

Table 3-5 Comparison of Actual Thickness and Design Thickness (Continued)

Ref. HOV	BV		ABS	
	t (mm)	Deviation (%)	t (mm)	Deviation (%)
Shinkai 6500	92.4	-20.45	103.2	-28.78
Alvin	62.9	-18.92	71.6	-28.77
Nautile	80.1	-22.6	90.4	-31.42
Consul	80.1	-11.36	90.4	-21.46
Jiaolong	94.4	-18.43	104.1	-26.03

Table 3-6 Comparison of Actual Thickness and Design Thickness (Continued)

Ref. HOV	LR		DNVGL	
	t (mm)	Deviation (%)	t (mm)	Deviation (%)
Shinkai 6500	76.7	-4.17	80.3	-8.47
Alvin	53.9	-5.38	53.6	-4.85
Nautile	68.5	-9.49	69.2	-10.4
Consul	68.5	3.65	69.2	2.6
Jiaolong	79.3	-2.9	82.1	-6.21

Table 3-7 Comparison of Actual Thickness and Design Thickness (Continued)

Ref. HOV	CCS	
	t (mm)	Deviation (%)
Shinkai 6500	78.4	-6.25
Alvin	53.2	-4.14
Nautile	66.9	-7.32
Consul	66.9	6.13
Jiaolong	77.6	-0.77

3.4 Summary

Specifically, Nautile is certified by BV. However, the actual thickness differs from the design thickness. It has also been proved that the actual scantling can be decided independently and without consideration of the scantling calculation that is based on classification rules. Generally, the shipyard will estimate the structural scantling based on the classification rules and standards, and the design results will be evaluated with the model test and nonlinear FE analysis (FEA). Even though the actually used thicknesses of Nautile does not match the theoretically estimated values, there is a possibility of acceptance as long as the analysis results are within reasonable limits.

To confirm whether the structural strengths of the five studied pressure shells meet the design requirements, the strength analysis of the existing pressure shell was performed with the FEA software ABAQUS. Based on the analyzed results, the strengths of the five pressure shells were confirmed, and the ultimate strength results of the design requirements, classification rules, and FEA, were compared.

References

- [1] S. Yuan, Q. Chen, and K. Ye: Simulation and Evaluation of Ultimate Strength Based Safety Factor for Titanium Alloy Spherical Pressure Hull, MARSTRUCT 2019, International Conference on Marine Structures, Dubrovnik, Croatia, May 2019.
- [2] B.-B. Pan and W. C. Cui, A Comparison of Different Rules for the Spherical Pressure Hull of Deep Manned Submersibles, Journal of Ship Mechanics, vol. 15, pp. 276-285, 2011.
- [3] S. Takagawa, D. Kiuchi, K. Takahashi, Y. Yamauchi, K. Inoue, and T. Nishimura: Design and Construction of Spherical Pressure Hull of SHINKAI 6500, Report of Japan Marine Science and Technology Center (JAMSTEC), Rep. 23, pp. 329–343 March 1990.
- [4] W. Cui: An Overview of Submersible Research and Development in China, Journal of Marine Science and Application, vol. 17, pp. 459-470, 2018.
- [5] United States Department of Defense: Metallic Materials and Elements for Aerospace Vehicle Structures, MIL-HDBK-5H, December 1998.

Chapter 4 Structural analysis

4.1 Introduction

This chapter introduces ABAQUS applied to the buckling analysis of geometrically perfect and imperfect spherical pressure shells. This research used ABAQUS, a simulation software, to verify the design results of each classification rule. In numerical simulation, the Riks method (hereinafter referred to as the "ABAQUS / Riks method") in ABAQUS was used to perform elastic-plastic buckling analysis to calculate the ultimate strength and eigenvalue mode of a non-ideal spherical pressure shell.

4.2 ABAQUS software

ABAQUS is a powerful finite element software for engineering simulation, which can solve problems ranging from relatively simple linear analysis to many complex nonlinear problems. ABAQUS includes a rich cell library that can simulate any geometric shape. ABAQUS software is a world-renowned finite element analysis software. Founded in 1978, HKS (now ABAQUS) in Botolph Claydon, Rhode Island, USA is the creator of the software. The main task of ABAQUS software is to analyze and calculate the nonlinear finite element model.

In recent years, ABAQUS users have also increased year by year, which has greatly promoted the development of ABAQUS software. With the continuous progress of basic theories and computer technology, ABAQUS is also gradually solving various technical problems in the software and improving the software, which has gradually become more perfect.

As one of the engineering software, ABAQUS software with its powerful finite element analysis function and CAE function is widely used in machinery manufacturing, civil engineering, tunnels and bridges, water conservancy and hydraulic engineering, automobile manufacturing, shipbuilding industry, aerospace, nuclear industry, petroleum Chemical, biomedical, military, civilian and other fields.

In these fields, corresponding static and quasi-static analysis, modal analysis, transient analysis, contact analysis, elastoplastic analysis, geometric nonlinear analysis, collision and impact analysis, explosion analysis, buckling analysis, fracture analysis can be effectively carried out In addition to structural analysis and thermal analysis such as fatigue and durability analysis, it can also perform thermo-structure coupling analysis, acoustic field and acoustic-structure coupling analysis,

piezoelectric and thermoelectric coupling analysis, fluid-structure coupling analysis, mass diffusion analysis, etc.

In addition to effectively solving various complex models and solving practical engineering problems, ABAQUS is also superior in analytical capabilities and reliability. In addition, ABAQUS has a rich cell library, which can simulate various complex geometric shapes, and a rich material model library, such as rubber, metal, reinforced concrete, etc., for users to choose from.

4.3 FEA overview

In addition to the buckling load, in the strength estimation of the pressure shell, the yield load also needs to be considered. In this research, the analysis process of the spherical pressure shell was divided into two parts: a) stress and b) stability analyses. The FE analysis process is shown in Figure 4-1. At the beginning of the process, a static stress analysis was carried out to verify the yield load, and any inelastic behavior of the material and imperfections are ignored. Secondly, the first-order instability mode was identified as the lowest buckling load and as the most critical load in the eigenvalue buckling analysis.

However, the actual buckling strength is usually much lower than the eigenvalue. It is well known that even small imperfections will reduce the overall strength and cause structural instability. To accurately estimate the ultimate strength of the pressure shell, an imperfection was introduced initially in the model to allow the conduct of elastic-plastic buckling analysis by the ABAQUS/Riks Method^[1].

The improved Riks method implemented in, performs geometric and material nonlinear analysis that includes imperfections. The actual buckling resistance can be obtained without adding any additional reduction factors^{[2][3]}.

The imperfection form is the first-order instability mode obtained based on the eigenvalue buckling analysis. In addition to the geometrical imperfections, during the elastic-plastic buckling analysis, the nonlinearity of the material can also be considered. Finally, the ultimate strength of the pressure shell was obtained. According to the strength assessment requirements, the yielding and ultimate buckling loads cannot be smaller than the design pressure P_d . The ABAQUS/Riks Method was used to perform the postbuckling analysis. This method can be used to analyze some discontinuous responses at the buckling point directly. The evaluation of the buckling load magnitude P_{total} by the Riks method is obtained with Equation 4-1.

$$P_{total} = P_0 + \lambda(P_{ref} - P_0) \quad (4-1)$$

where P_0 is the dead load that is defined at the beginning of the step and is never redefined. P_{ref} is the reference load defined in the Riks step, and λ is the load proportionality factor. Riks analysis is usually the loading analysis corresponding to the first-order buckling eigenvalue. In this research, the maximum allowed out-of-circularity ΔR value was used as the initial imperfection of the pressure shell to introduce elastic-plastic buckling analysis to obtain the corresponding buckling mode. The out-of-circularity is the deviation between the actual measurement radius R' and average radius \bar{R} . According to the DNVGL and CCS rules, the deviations of the horizontal Δx and vertical Δy measured from the assumed center could not exceed 0.5% of the mean radius. Figure 4-2 shows a schematic of the measured out-of-circularity.

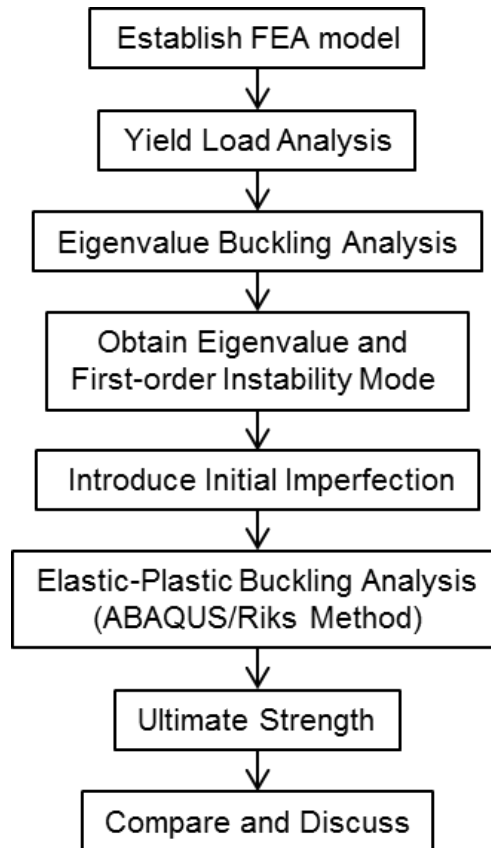


Fig. 4-1 Process Chart Used for the Analysis of the Ultimate Strength

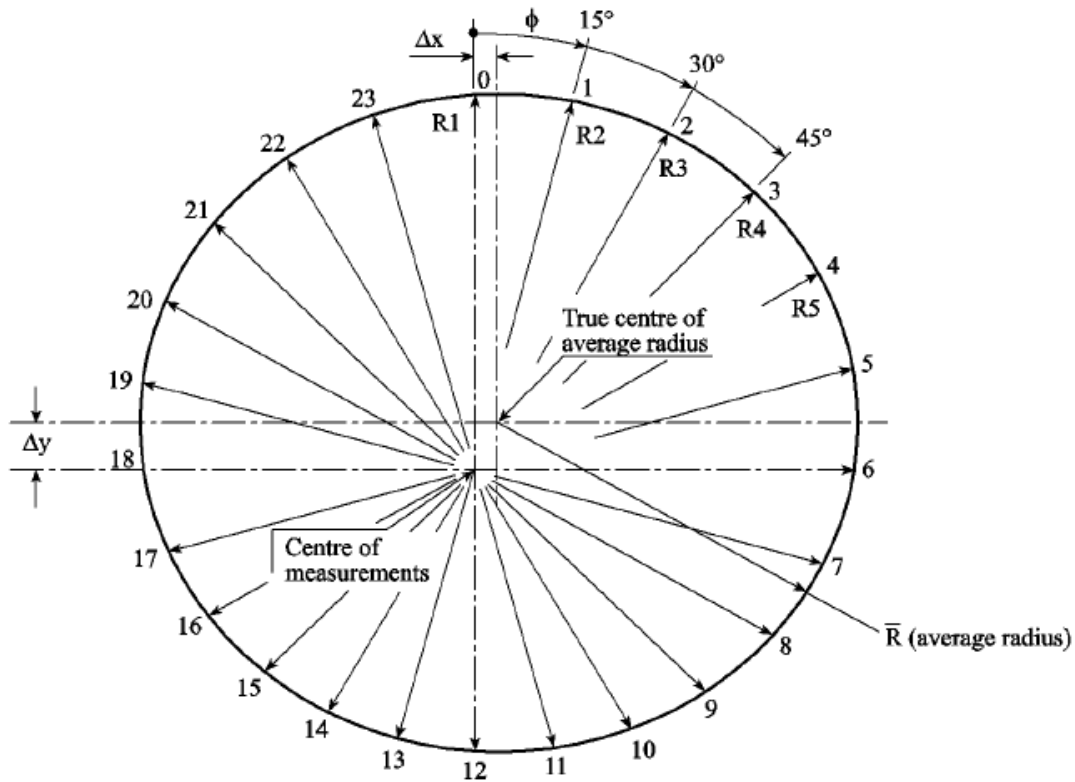


Fig. 4-2 Measured Schematic of the Out-of-circularity

4.2.1 Finite element modeling

The finite element modeling is done in the finite element software package Abaqus 6.12 (product of Dassault Systems). Numerical software packages use a series of discrete points to solve problems. Each point or node adds a degree of freedom (DOF) to the system. Therefore, the more degrees of freedom in the model, the better it can capture structural behavior. Finite element analysis does not take much time to produce results. However, to make the result accurate, we must prove that the result converges to a solution and is independent of the mesh size. Mesh refinement is essential to increase the accuracy of the analyzed results [4].

In this research, a convergence evaluation was conducted to analyze the spherical pressure shell to obtain mesh-independent results. The mesh size convergence analysis results of the five pressure shells are shown in Figure 4-3 and Tables 4-1 to 4-5. According to the mesh convergence studies, the degree of freedom of the numerical model needs to be improved by the procedure of mesh refinement. When the convergence ratio of the deformation is less than 0.5%, the grid of the previous order can be selected.

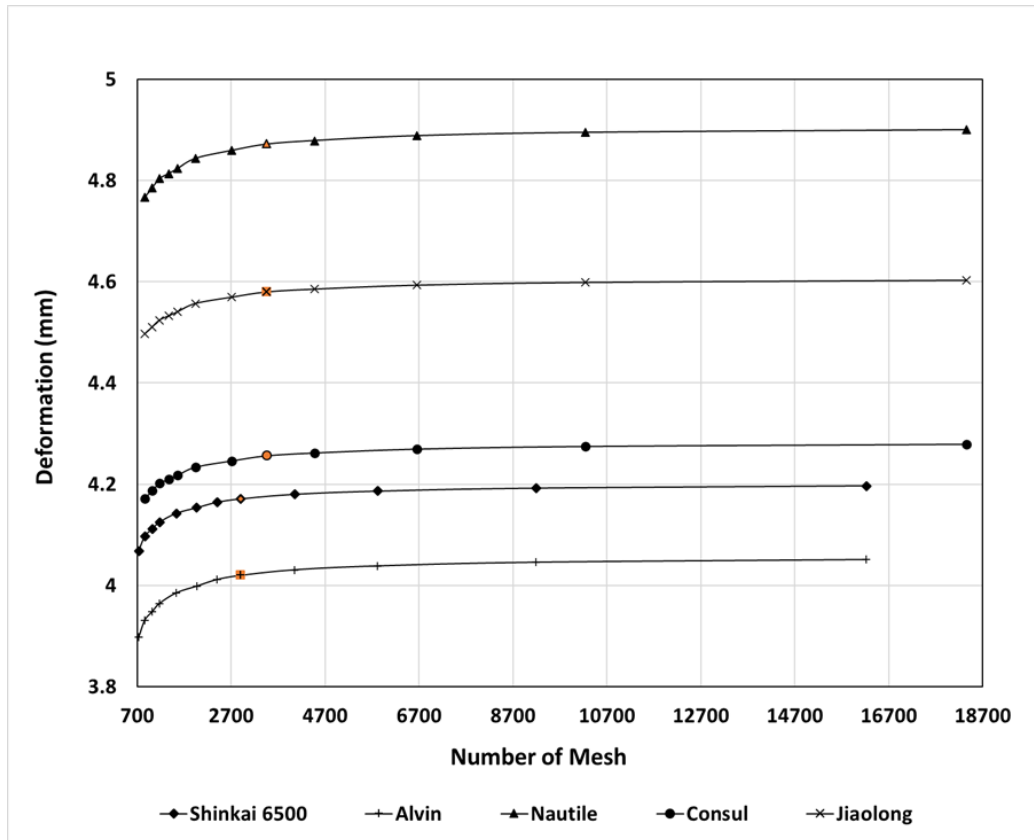


Fig. 4-3 The Mesh Size Convergence Analysis Results

Table 4-1 Mesh Convergence Results of Shinkai 6500

Mesh Size	Number	Deformation	Convergence Ratio
30	16224	4.19692	0.00
40	9192	4.19242	0.11
50	5816	4.18639	0.25
60	4056	4.18009	0.40
70	2904	4.17102	0.62
80	2400	4.1643	0.78
90	1968	4.15346	1.04
100	1536	4.14262	1.29
110	1176	4.12498	1.71
120	1020	4.111145	2.04
130	864	4.09731	2.37
140	736	4.0683	3.06

Structural analysis

Table 4-2 Mesh Convergence Results of Alvin

Mesh Size	Number	Deformation	Convergence Ratio
30	16224	4.05121	0.00
40	9192	4.04584	0.13
50	5816	4.03856	0.31
60	4056	4.03089	0.50
70	2904	4.01986	0.77
80	2400	4.0117	0.98
90	1968	3.998595	1.30
100	1536	3.98549	1.62
110	1176	3.9644	2.14
120	1020	3.947945	2.55
130	864	3.93149	2.96
140	736	3.89771	3.79

Table 4-3 Mesh Convergence Results of Nautila

Mesh Size	Number	Deformation	Convergence Ratio
30	18358	4.90017	0.00
40	10238	4.89492	0.11
50	6654	4.88832	0.24
60	4470	4.87882	0.44
70	3456	4.87173	0.58
80	2718	4.85952	0.83
90	1944	4.84384	1.15
100	1560	4.823775	1.56
110	1368	4.8137425	1.76
120	1176	4.80371	1.97
130	1020	4.785435	2.34
140	864	4.76716	2.71

Structural analysis

Table 4-4 Mesh Convergence Results of Consul

Mesh Size	Number	Deformation	Convergence Ratio
30	18358	4.27939	0.00
40	10238	4.27515	0.10
50	6654	4.26981	0.22
60	4470	4.26214	0.40
70	3456	4.25654	0.53
80	2718	4.24654	0.77
90	1944	4.23415	1.06
100	1560	4.21798	1.44
110	1368	4.209895	1.62
120	1176	4.20181	1.81
130	1020	4.18703	2.16
140	864	4.17225	2.50

Table 4-5 Mesh Convergence Results of Jiaolong

Mesh Size	Number	Deformation	Convergence Ratio
30	18358	4.60367	0.00%
40	10238	4.5993	0.09%
50	6654	4.59381	0.21%
60	4470	4.58592	0.39%
70	3456	4.58025	0.51%
80	2718	4.57	0.73%
90	1944	4.55732	1.01%
100	1560	4.540735	1.37%
110	1368	4.5324425	1.55%
120	1176	4.52415	1.73%
130	1020	4.510351381	2.03%
140	864	4.496552762	2.33%

According to the convergence results of the five studied pressure shells, the difference in the deformation value was small for the element sizes of 70 mm and

60 mm. To reduce the calculation time, the average element size of 70 mm was used in the pressure-shell analysis. The meshing of the spherical pressure shell of Shinkai 6500 and Alvin yielded 2904 elements, and Nautila, Consul, and Jiaolong yielded 3456 elements.

The shell element S4R was used to avoid hourglasses. In the case of linear elastic buckling analysis, mesh convergence analysis is used to determine the number of elements. Note that different shell thicknesses may result in different critical element numbers. Nevertheless, in order to maintain uniformity and simplify the problem, according to the mesh convergence analysis of the shell, the maximum number of elements in the shell with different wall thicknesses is used in each model. The FE model of the spherical shell is shown in Figure 4-4.

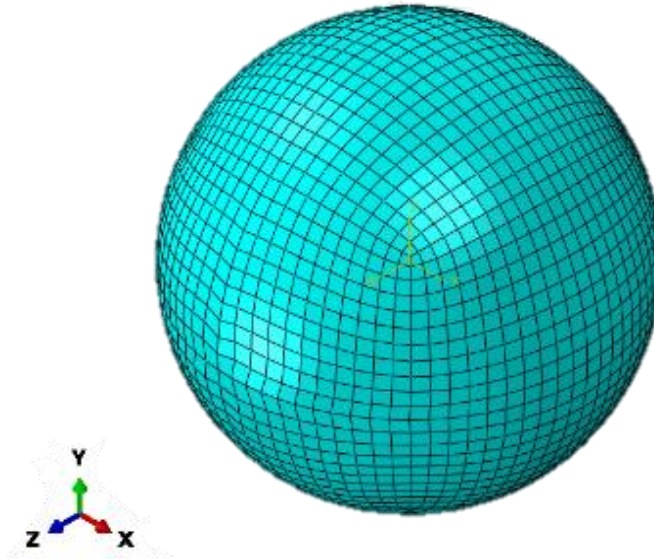


Fig. 4-4 Finite Element Model of Spherical Shell

4.2.2 Boundary conditions

The design pressure was used as the outer, uniform external pressure in the spherical shell, $p=1$ MPa. In this way, the characteristic value obtained by linear elastic buckling analysis directly corresponds to the linear buckling load, while the arc length value obtained from the geometric and material nonlinear analysis is the nonlinear buckling load. When the analysis of the entire pressure shell was performed, the boundary conditions were set at the position at which the major axes intersected, whereby all the degrees-of-freedom were constrained. To avoid rigid body motion, given that the load was applied separately on the outer shell, the

deformations in the radial directions are allowed. The settings of the parameters for the FEA model are shown in Figure 4-5.

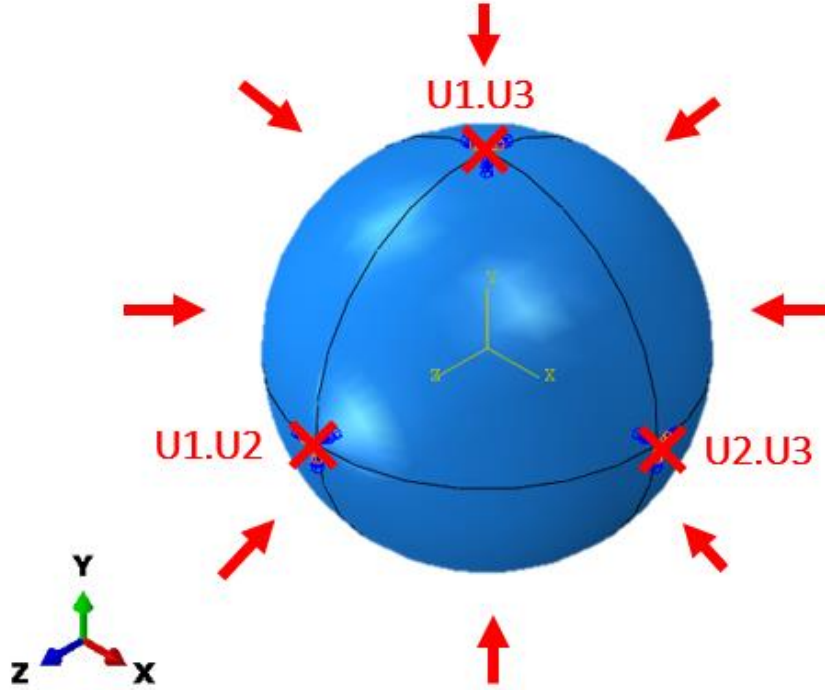


Fig. 4-5 Loading Case and Boundary Conditions

4.2.3 Verification

The verification of the FEA results is a vital process used to ensure that the simulation results are reliable and valid in real situations. Before the onset of the analysis, three experimental models were selected for the verification in this research, including the MT-1 ^[5], HY-105 ^[6], and t0.4-1 models ^[7]. The FEA calculation was performed under the same design conditions, and the analysis results were compared with the experimental results to verify the accuracy of the FEA calculation method in this research. The test model characteristics are listed in Table 4-6.

According to the above method, the structure analysis of 3 pressure spherical shells is carried out, and the calculation results are shown in Table 4-2 to Table 4-4. It can be observed that the deviation between the analysis and test is small (does not exceed 4%), and the collapse modality is also consistent. It was confirmed that the analysis method and process used in this research have high accuracies, and can accurately simulate the buckling behavior of pressure shells with imperfections. Therefore, the pressure shell analysis can be performed with the analytical method proposed in this research.

Table 4-6 The test model characteristics

Test Model	Yokota et al. MT-1	Kanai et al. HY-105	Zhang et al. t0.4-1
Material	Titanium Alloy	HT-100	304 Stainless Steel
Nominal Radius (mm)	242	250	75
Thickness (mm)	16	10	0.4

According to the above method, the structure analysis of 3 pressure spherical shells is carried out, and the calculation results are shown in Table 4-7 to Table 4-9. It can be observed that the deviation between the analysis and test is small (does not exceed 4%), and the collapse modality is also consistent. It was confirmed that the analysis method and process used in this research have high accuracies, and can accurately simulate the buckling behavior of pressure shells with imperfections. Therefore, the pressure shell analysis can be performed with the analytical method proposed in this research.

Table 4-7 Verification Results of MT-1 for the FEA Calculation Method

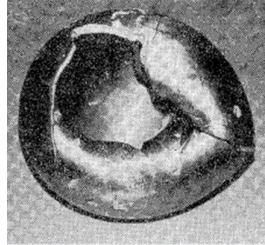
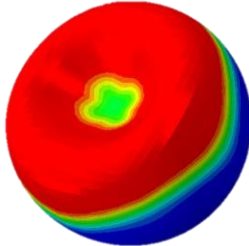
Test Collapse Modality ^[5]	
Test Collapse Load	120.62 MPa
ABAQUS Collapse Modality (By this research)	
ABAQUS Collapse Load (By this research)	116.124 MPa
Deviation	3.73%

Table 4-8 Verification Results of HY-105 for the FEA Calculation Method


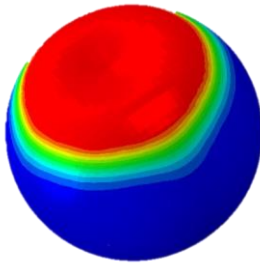

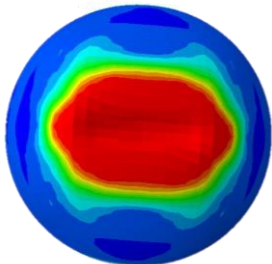
Test Collapse Modality ^[6]	
Test Collapse Load	81.4 MPa
ABAQUS Collapse Modality (By this research)	
ABAQUS Collapse Load (By this research)	80.4 MPa
Deviation	1.23%

Table 4-9 Verification Results of t0.4-1 for the FEA Calculation Method

Test Collapse Modality ^[7]	
Test Collapse Load	1.71 MPa
ABAQUS Collapse Modality (By this research)	
ABAQUS Collapse Load (By this research)	1.65 MPa
Deviation	3.51%

4.4 Analysis of spherical pressure shell

4.4.1 The yield load analysis

When the membrane stress in the spherical shell reaches the yield point of the material, it is regarded to be the maximum allowable stress. The yield point is the first stress in the material, which is less than the maximum available stress.

The yield load analysis results of the five existing pressure shells are listed in Table 4-10 and Table 4-11. The theoretical solution of the yield load is calculated by Equation 2-2. The comparison between the theoretical and analyzed results shows that the deviation is small (does not exceed 4%).

The yield load at which the membrane stress in the spherical shell reaches the yield point of the material has exceeded the design pressure by far. Stress analysis confirmed that there was a substantial design margin associated with the studied pressure shells. However, this result only considers the membrane yield stress of the spherical pressure shell under uniform external pressure.

As we all know, in the design of the spherical pressure shell, it is necessary to clearly confirm the ultimate strength of the spherical pressure shell. Therefore, in the next section, we will focus on the buckling analyzed results of five spherical pressure shells under uniform external pressure.

Table 4-10 Analysis Results of Yield Load

	Shinkai 6500	Alvin	Nautille
Theoretical Yield Load (MPa)	112.01	78.58	100.03
Analytical Yield Load (MPa)	116.20	80.62	103.06
Deviation (%)	3.74	2.60	3.03
Design Pressure (MPa)	101.31	67.87	90.50
Design Margin (%)	14.70	18.78	13.88

Table 4-11 Analysis Results of Yield Load (Continued)

	Consul	Jiaolong
Theoretical Yield Load (MPa)	114.07	123.4
Analytical Yield Load (MPa)	117.43	127.6
Deviation (%)	2.94	3.45
Design Pressure (MPa)	90.5	105.6
Design Margin (%)	29.76	20.88

4.4.2 The eigenvalue buckling analysis

The linear eigenvalue buckling analysis in Abaqus is based on linear perturbations and predicts the strength (bifurcation point) of a buckling ideal linear elastic member. In the analysis of linear elastic eigenvalue buckling, we search for loads where the stiffness matrix of the model becomes singular. This type of analysis predicts the theoretical buckling strength of an elastic structure, where the buckling load is calculated relative to the bottom of the member. Generally, material stiffness is positive definite, while geometric stiffness can allow negative values for certain modes, depending on the applied load. The influence of negative geometric stiffness will cause the overall tangent matrix of the member to be single, resulting in buckling.

However, nonlinearities and imperfections often prevent most members from achieving their theoretical elastic buckling strength. Therefore, linear elastic eigenvalue analysis usually produces too many results, so the eigenvalue buckling load factor is somewhat overestimated. Non-linear static analysis includes defects and elastoplastic material properties, which can get more accurate results.

In the eigenvalue buckling analysis, the eigenvalue is the theoretical critical buckling load, and the corresponding eigenvector is the buckling mode. Figure 4-6 to Figure 4-10 show the results of the first-order instability mode and Table 4-7 lists the eigenvalue buckling load.

For practical purposes, the minimum critical load corresponding to the first and second buckling modes is the most important result, because the buckling modes are reported in ascending order according to their values. It is important to note that the

geometric stiffness matrix is only based on component forces, so any pre-buckling rotation effects due to moments are ignored in this analysis. The eigenvalue analysis provides the factor by which the load must be multiplied to reach the buckling load. The applied load step is set to 1 MPa and the eigenvalue of mode 1 of Shinkai 6500 is 766.52 MPa. The magnitude of the pressure applied is not important, since it will be scaled by the eigenvalues. The estimated maximum load, for each of the test parts, which can be supported prior to structural instability according to the linear eigenvalue analysis, is to be found in Table 4-12.

Consider the results from Shinkai 6500 as an example. The buckling load for Shinkai 6500 based on the simulations is 766.52 MPa. This buckling load is about 75% higher than inelastic behaviors of the material and imperfections are ignored in the eigenvalue buckling analysis. Therefore, this buckling water depth is only established in ideal structural conditions that cannot be achieved when the actual structure is used.

In fact, the calculation results of first-order instability mode were far lower than the numerical solutions under deterministic imperfection. Non-linearities and imperfections tend to prevent most members from achieving their theoretical elastic buckling load. Therefore, linear elastic eigenvalue analysis usually produces too many results, so the eigenvalue buckling load factor is somewhat overestimated. To obtain a more accurate ultimate strength of the pressure shell, an initial imperfection is introduced in the model to conduct the elastic-plastic buckling analysis.

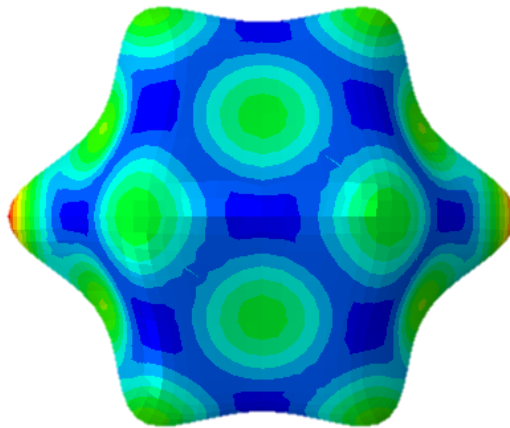


Fig. 4-6 First-order Instability Mode of Shinkai 6500

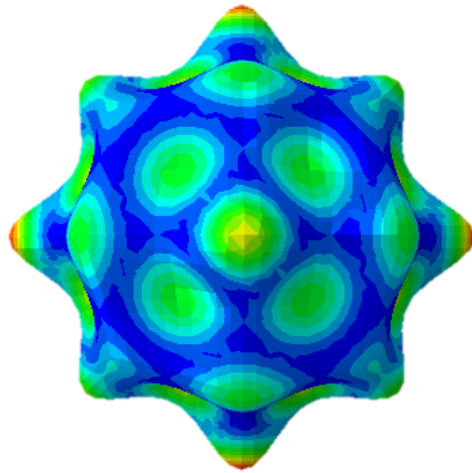


Fig. 4-7 First-order Instability Mode of Alvin

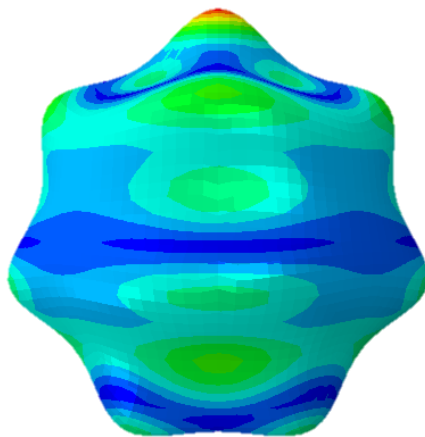


Fig. 4-8 First-order Instability Mode of Nautil

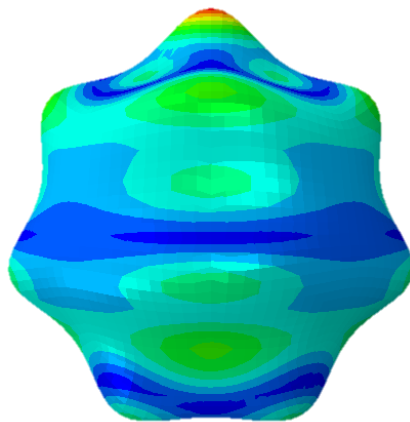


Fig. 4-9 First-order Instability Mode of Consul

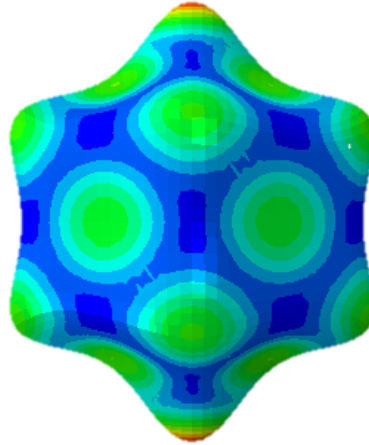


Fig. 4-10 First-order Instability Mode of Jiaolong

Table 4-12 Analysis Results of Eigenvalue Buckling

	Shinkai 6500	Alvin	Nautile	Consul	Jiaolong
Analytical Buckling Load (MPa)	766.52	370.24	495.01	651.7	766.93

4.4.3 The elastic–plastic buckling analysis

Linear eigenvalue analysis may be sufficient for design verification, but due to material nonlinearity and geometric nonlinearity, load reflection analysis will be used to further study the model. The buckling load predicted by the linear eigenvalue analysis yields to the high value of the critical load because plastic deformation or material failure occurs before that point. The buckling load is calculated relative to the basic state of the model. This research conducted two nonlinear static analysis; nonlinear static large deformation buckling analysis and nonlinear static Riks buckling analysis.

This research used the ABAQUS/Riks Method for the elastic–plastic buckling analysis. In this analysis, the out-of-circularity was introduced in the first-order mode of the eigenvalue buckling analysis as the initial imperfection to obtain the ultimate buckling load, and represents the ultimate strength of the pressure shell. When the imperfections are introduced, the ultimate buckling strength of the pressure shell would be reduced, and the structural stiffness would become worse.

The buckling paths of the five pressure shells studied herein based on the elastic–plastic buckling analysis is illustrated in Figures 4-11 to 4-15. These figures show

the applied pressure and the displacement results. It can be observed that the applied pressure increased as a function of deflection. This situation continued to the critical point of the structural collapse. Subsequently, the path leveled off.

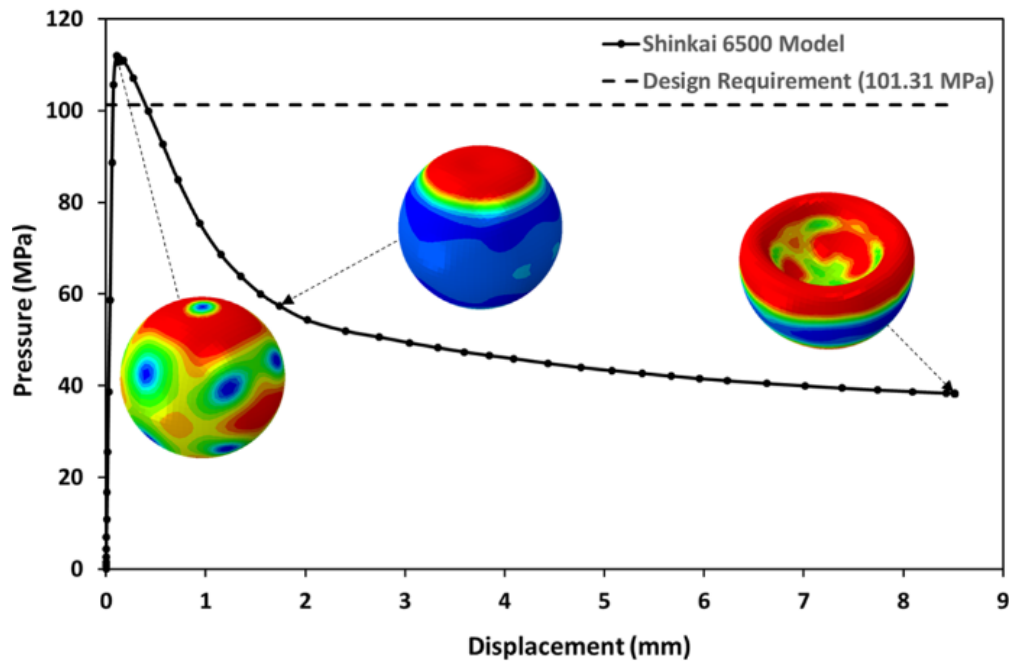


Fig. 4-11 Pressure Displacement Path Proposed by Shinkai 6500

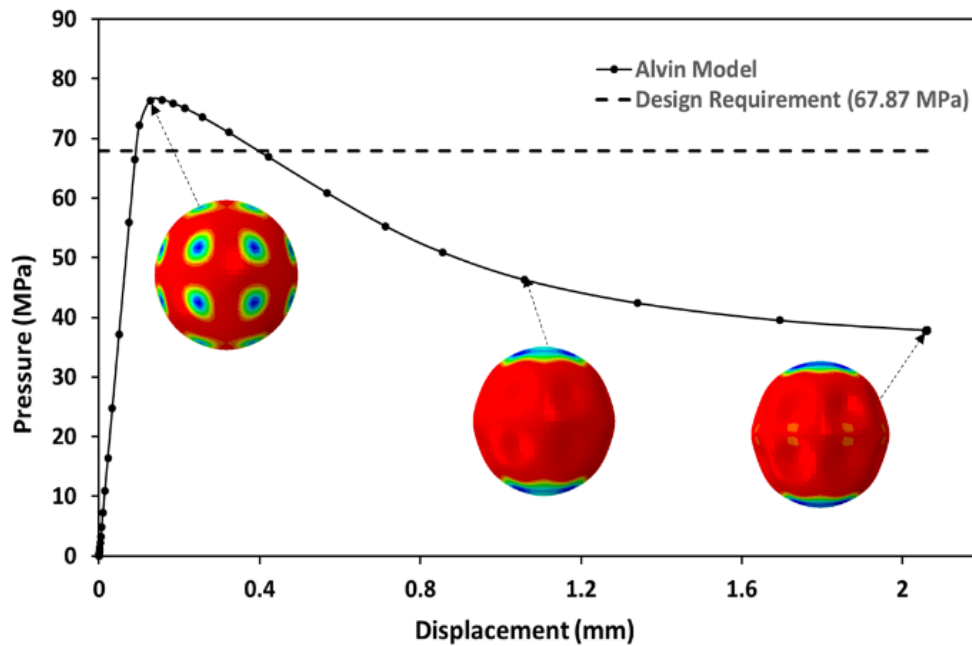


Fig. 4-12 Pressure Displacement Path Proposed by Alvin

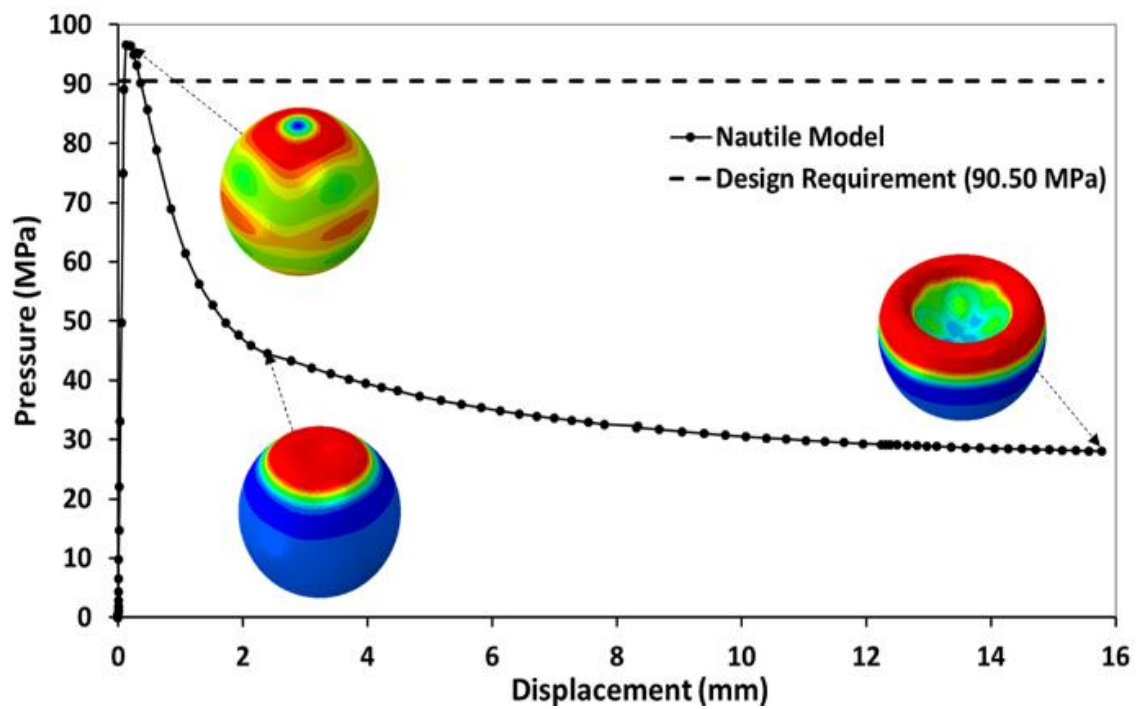


Fig. 4-13 Pressure Displacement Path of Nautil

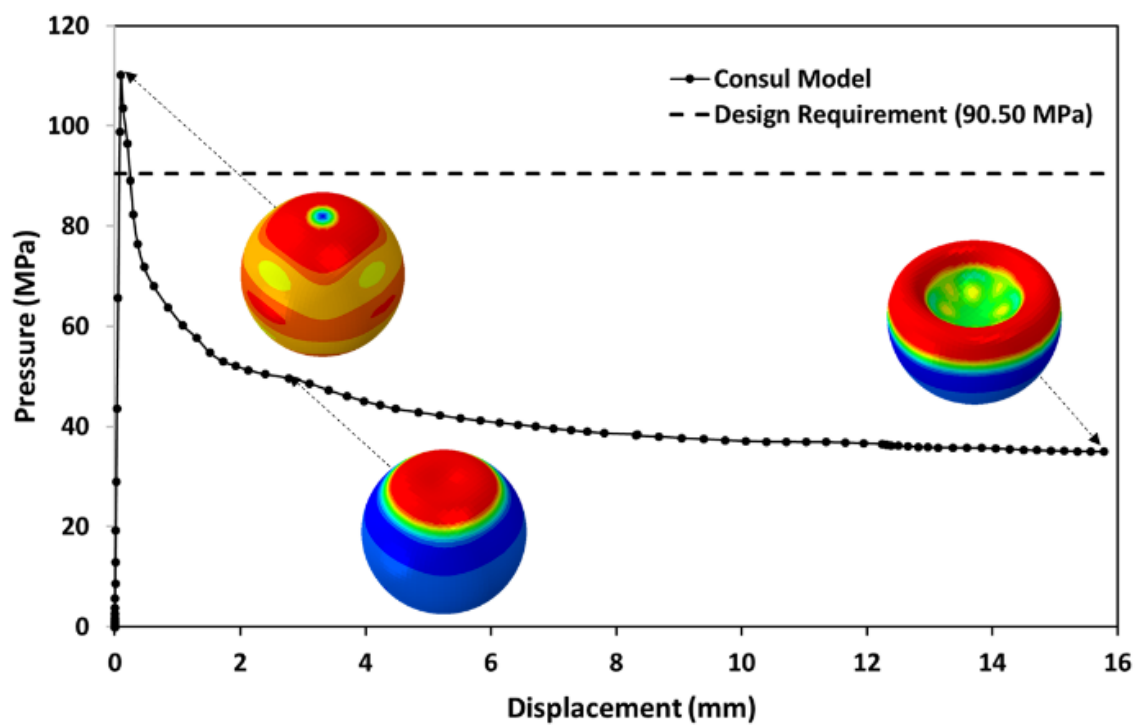


Fig. 4-14 Pressure Displacement Path of Consul

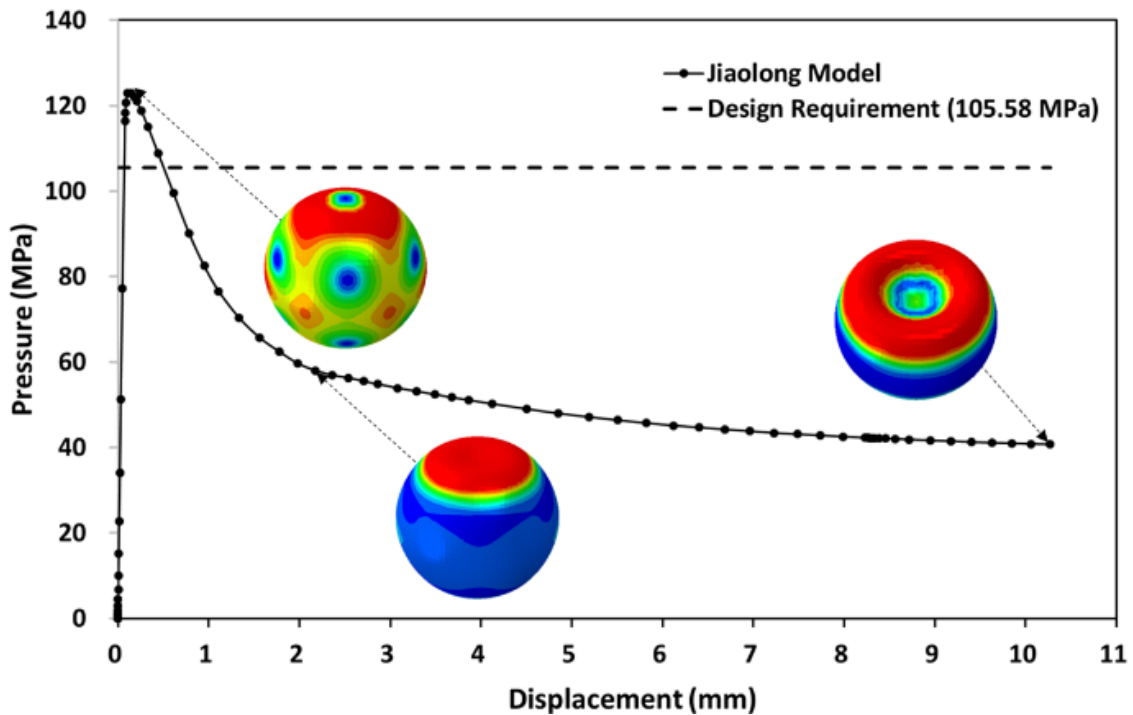


Fig. 4-15 Pressure Displacement Path of Jiaolong

Table 4-13 and Table 4-14 presents comparable results related to the elastic–plastic buckling analysis. The analyzed results show that the overall strength and stiffness will be affected by structural defects. Accordingly, the ultimate strength is only approximately 15-20% of the elastic buckling load. At this time, the ultimate strength is very close to the real state. It is determined that the five studied pressure shells meet the design requirements and do not impose any safety concerns.

Table 4-13 Analyzed Results of Elastic–Plastic Buckling

	Shinkai 6500	Alvin	Nautile
R_m (mm)	1036.75	1025.5	1081
ΔR (mm)	5.18375	5.1275	5.405
Design Pressure P_d (MPa)	101.31	67.87	90.50
Ultimate Strength P_u (MPa)	112.00	76.48	96.60
Design Margin (%)	10.56	12.69	6.74

Table 4-14 Analyzed Results of Elastic–Plastic Buckling (Continued)

	Consul	Jiaolong
R_m (mm)	1085.5	1088.5
ΔR (mm)	5.4275	5.4425
Design Pressure P_d (MPa)	90.50	105.58
Ultimate Strength P_u (MPa)	110.17	122.15
Design Margin (%)	21.74	15.69

4.5 Summary

In the present chapter, the results of analytical and numerical study into the buckling and post-buckling performance of five titanium alloy spherical pressure shells were presented, along with three laboratory scale spherical shells for validation. The conclusions are as follows:

- (1) According to the comparison results listed above, the ultimate strengths of the existing pressure shells met the requirements.
- (2) Reducing the thickness is advantageous for the structure of the pressure shell because of the lighter weight and the improved overall performance of the structure. It is thus recommended to reduce the thickness to reduce the overall weight.
- (3) Table 4-15 to Table 4-18 shows the comparison of the ultimate strength outcomes between the rule design and FEA. It can be inferred that the design that was based on LR rules can yield more stable results, and the deviation is smaller than other rules.

Table 4-15 Deviations of Ultimate Strength of FEA for Different Rules

Ref. HOV	RS		DNV	
	P_u' (MPa)	Deviation (%)	P_u' (MPa)	Deviation (%)
Shinkai 6500	102.15	9.64	97.01	15.45
Alvin	67.67	13.01	58.19	31.44
Nautilus	87.82	9.99	75.77	27.48
Consul	102.36	7.63	90.67	21.51
Jiaolong	111.93	9.13	100.61	21.41

Structural analysis

Table 4-16 Deviations of Ultimate Strength of FEA for Different Rules (Continued)

Ref. HOV	BV		ABS	
	P_u' (MPa)	Deviation (%)	P_u' (MPa)	Deviation (%)
Shinkai 6500	82.13	36.37	70.06	59.87
Alvin	53.03	44.23	44.75	70.92
Nautile	68.31	41.42	57.7	67.41
Consul	79.87	37.93	68.34	61.22
Jiaolong	87.05	40.33	75.32	62.17

Table 4-17 Deviations of Ultimate Strength of FEA for Different Rules (Continued)

Ref. HOV	CCS		LR	
	P_u' (MPa)	Deviation (%)	P_u' (MPa)	Deviation (%)
Shinkai 6500	124.58	-10.09	104.5	7.18
Alvin	61.99	23.37	70.39	8.65
Nautile	76.48	26.32	89.93	7.42
Consul	103.55	6.39	103.25	6.71
Jiaolong	125	-2.28	112.35	8.72

Table 4-18 Deviations of Ultimate Strength of FEA for Different Rules (Continued)

Ref. HOV	DNVGL	
	P_u' (MPa)	Deviation (%)
Shinkai 6500	93.61	19.65
Alvin	63.57	20.3
Nautile	81.96	17.86
Consul	92.74	18.79
Jiaolong	99.78	22.41

References

- [1] ABAQUS Analysis User's Manual: 6.2.4 "Unstable Collapse and Postbuckling Analysis".
- [2] H. Schmidt: Stability of Steel Shell Structures: General Report, Journal of Constructional Steel Research, vol. 55, no. 1-3, pp. 159-181, July 2000.
- [3] J. Lund: Buckling of cylindrical members with respect to axial loads, Norwegian University of Science and Technology, June 2014.
- [4] P. Jasion, K. Magnucki: Elastic Buckling of Clothoidal-Spherical Shells Under External Pressure - Theoretical Study, Thin-Walled Structures, vol. 86, pp. 18-23, 2015.
- [5] T. Shinohara, S. Takagawa, K. Yokota, H. Morihana, Y. Yamauchi, and K. Urugami: Collapse Strength of Spherical Pressure Hull for Deep Submergence Research Vehicle Made of Titanium Alloy, Journal of the Kansai Society of Naval Architects, Vol. 198, pp. 109-119 September 1985.
- [6] K. Kanai, H. Morihana, T. Yamasaki, and K. Terada: Experimental Investigation on the Collapse Strength of Spherical Shells, The Japan Society of Naval Architects and Ocean Engineers, Vol. 1972, No.132, pp. 269-279, October 1972.
- [7] J. Zhang, M. Zhang, W. Tang, W. Wang, and M. Wang: Buckling of Spherical Shells Subjected to External Pressure: A Comparison of Experimental and Theoretical Data, Thin-Walled Structures, Vol. 111, pp. 58-64, February 2017.

Chapter 5 Proposal

5.1 Discussion

When spherical pressure shells are exposed to external pressure, this may cause yield or buckling collapse responses. Assuming that yield and buckling collapses occur simultaneously, Equations 2-2 and 2-3 become the same, and Equation 5-1 can be derived.

$$\frac{\sigma_y \sqrt{3(1-\nu^2)}}{E} = \frac{t}{R_m} \quad (5-1)$$

According to Equation 5-1, Ti-6Al-4V ELI, Ti-6211 and Ti-6Al-4V were used as the design material. The comparison between P_y and P_e is shown in Figure 5-1 to 5-3. It can be observed that when the ratio of the thickness to the radius (t/R_m) is small, P_y is always greater than P_e . The mean of the buckling load is less than the yield load; subsequently, the pressure shell fails owing to buckling before the yield stress is reached. However, as the value of t/R_m increases, P_e will become greater than the yield load and will grow faster.

When the t/R_m value is small, the pressure shell mainly collapses by buckling. On the contrary, as the value of t/R_m increases, the pressure shell mainly collapses owing to the yield load. The ultimate strength results for the five pressure shells are also shown in Figure 5-1 to 5-3. The spherical shell can withstand considerable pressure after the first yield. If buckling occurs before the yield, the critical pressure values are expected to be underestimated.

In the elastic-plastic analysis, the ultimate buckling load is always larger than yield load. Effectively, this means that the yield would occur first. The elastic-plastic analysis results confirmed that the ultimate strengths of the five pressure shells were all close to the yield load.

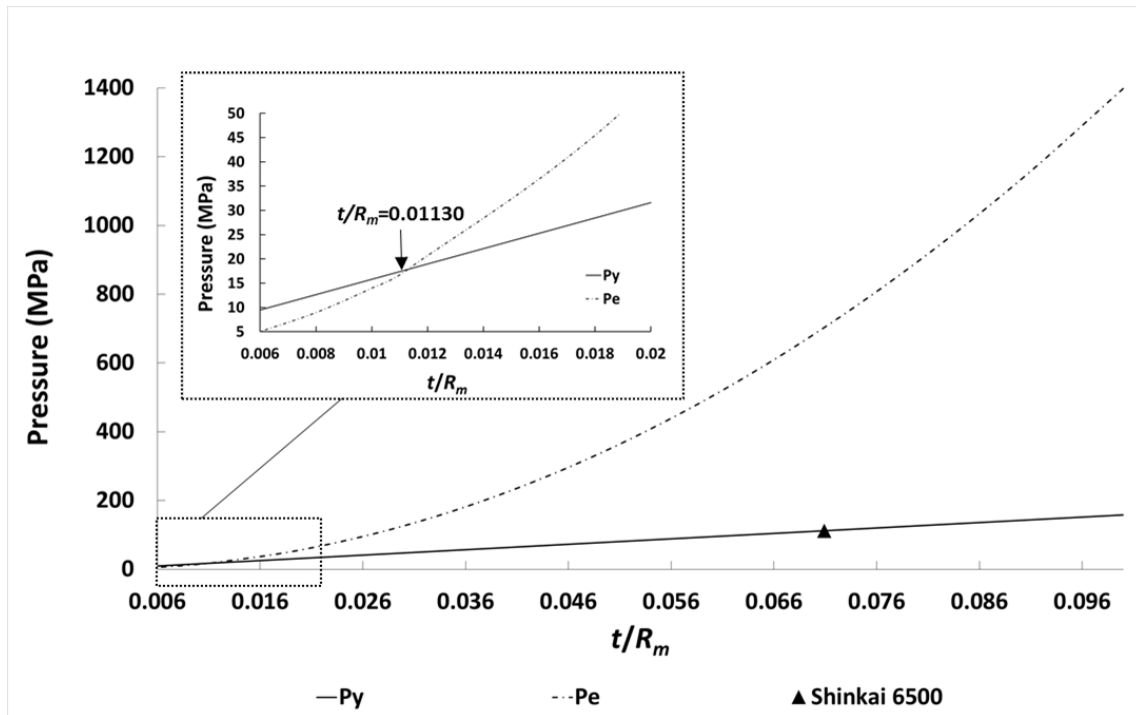


Fig. 5-1 Comparison Between P_y and P_e (Ti-6Al-4V ELI)

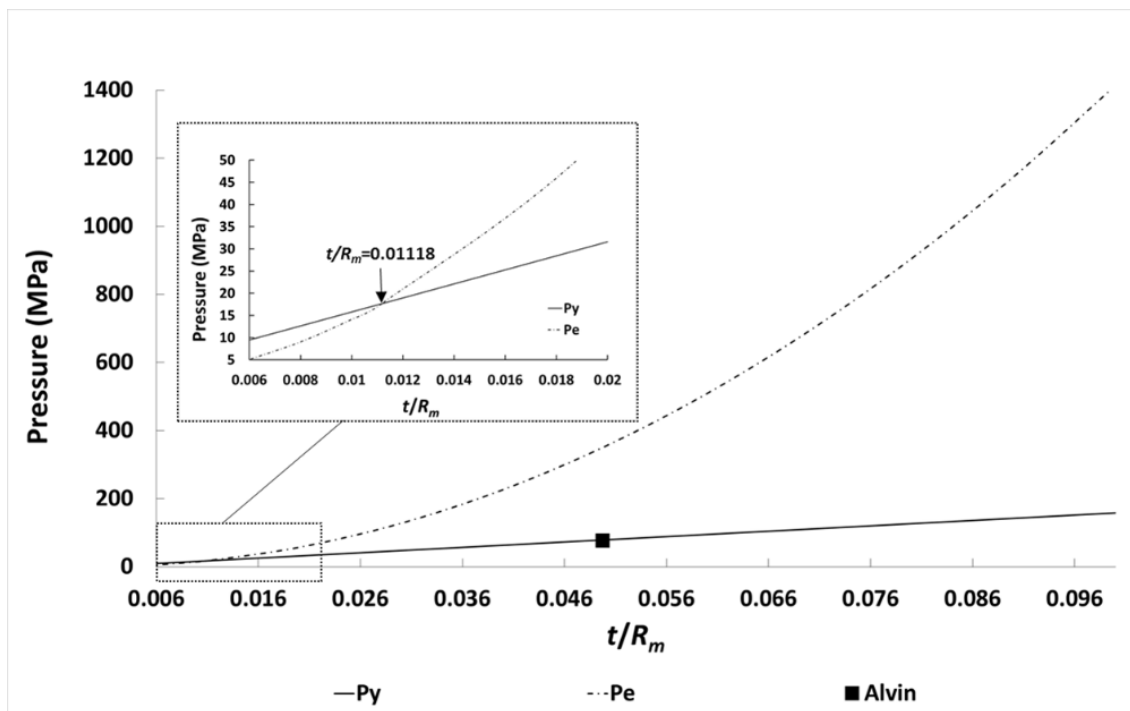


Fig. 5-2 Comparison Between P_y and P_e (Ti-6211)

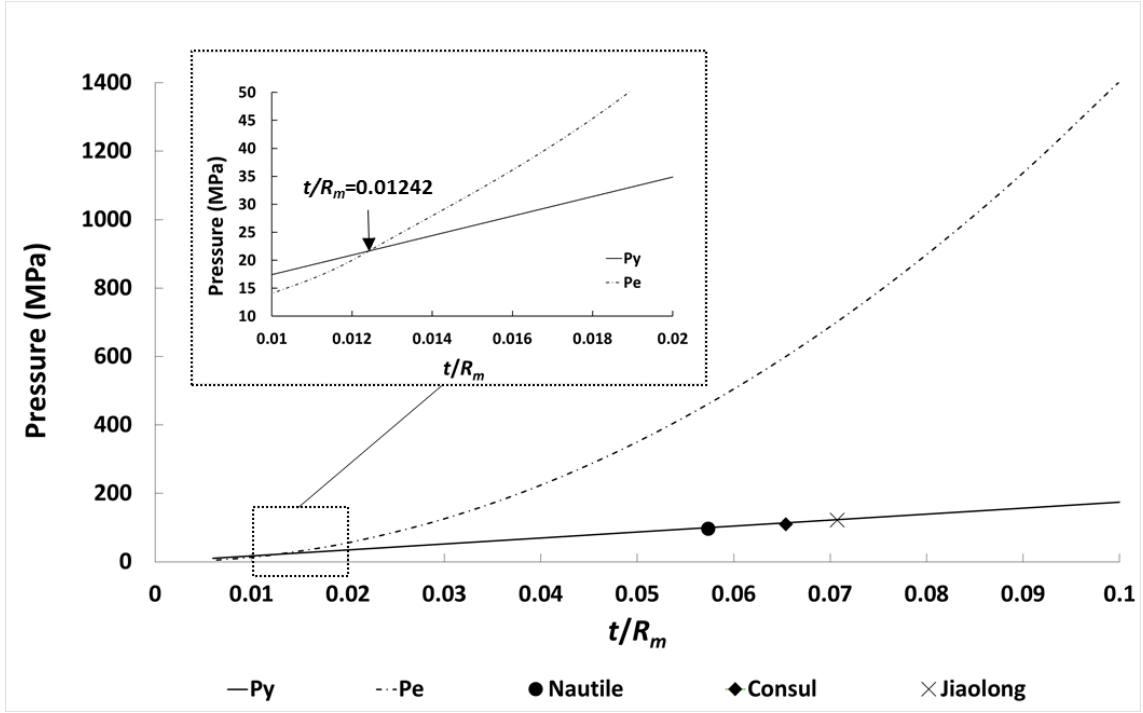


Fig. 5-3 Comparison Between P_y and P_e (Ti-6Al-4V)

5.2 Proposal of the pressure shell design

As mentioned in the introduction, all current design rules are based on the classic yield load formula and theoretical elastic buckling formula, but there are subtle differences between different rules. DNVGL rules are based on these two formulae for pressure shell strength evaluation of a pressure shell. DNV, BV, and CCS consider both yield load and elastic buckling load and use the minimum values of these loads as the ultimate strength. The safety factor is considered in the calculation of the yield load, and the structural imperfection factor is considered in the calculation of the elastic buckling load.

The DNV rules are mainly based on the classic yield load formula for strength evaluation, and the strength loss caused by structural imperfections is also considered. RS and ABS rules divide the design method based on two collapse problems. In the first stage, when t/R is small, the pressure shell mainly collapses due to buckling. Generally thin spherical shells belong to the first stage. In the second stage, as t/R increases, the pressure shell mainly collapses due to yielding, which means that the stresses in the spherical shell reach the yield strength of the material. In the LR rules, material coefficients are considered when evaluating structural stability.

Moreover, among all the rules, only ABS and RS rules clearly stipulates that its formula can be used for the calculation of titanium structures; other rules should only be applied to steel structures, and titanium structures should be considered as a special case.

Accurately estimating the effect of the initial imperfections on the structural stability is considerably difficult during the initial design phase of the spherical pressure shell. Additionally, there are clear differences between the design methods of each classification rule because the design coefficients are different. Although the LR rules can yield more accurate and stable estimation results, the method does not provide related design curves and coefficients in the strength evaluation process, and the design result are relatively conservative.

This research suggests that the use of the LR rules during the pressure-shell design phase for calculating the yield load and the buckling load can segregate the collapse into two stages. When the influence of the geometry, safety factor, and material used are considered, the lower bound curve of the BSI specification can be used in the design, as shown in Figure 2-4. In the subsequent section, this method is used to recalculate the thickness of the five pressure shells, and its effectiveness is discussed based on FEA.

5.3 Results of the proposed design method

According to the proposed design method, the thicknesses of the five pressure shells were recalculated, and the structural strengths were verified based on FEA. The thicknesses shown in Table 5-1 are the results obtained after calculation according to the lower bound curve of the BSI standard. The difference between this result and the required thickness calculated based on the LR rule (Table 3-6) is approximately 5–8%. This also proves that the design result of LR is relatively conservative. According to the comparison results, the thickness of the pressure shell calculated using the proposed design method was significantly lower than that calculated based on the original design rules and is close to the actual thickness. The structural geometry and design conditions of Nautile and Consul are the same, but a large design margin is used in the actual design of Consul.

The FEA results and design margin of the ultimate strength are listed in Table 5-2. Although the thickness was reduced, the structural strength was maintained within a safe range and satisfied the design requirements. According to the analysis results, the design method proposed herein can maintain a design margin of about 10% under

Proposal

different pressure shell geometries. This design margin can compensate for the loss that will occur during subsequent maintenance. The results confirmed that our proposed design method yields accurate and stable results. The calculation sheet of the proposed design method is listed in the appendix I to appendix V.

Table 5-1 Calculated Proposal Thickness Results

	Actual Thickness t_{ac} (mm)	Design Thickness t (mm)	Deviation (%)
Shinkai 6500	73.5	72.4	-1.50
Alvin	51.00	49.9	-2.15
Nautile	62.00	63.1	1.77
Consul	71.00	63.1	-11.13
Jiaolong	77.00	72.8	-5.45

Table 5-2 Comparison of Ultimate Strength Results

	Shinkai 6500	Alvin	Nautile	Consul	Jiaolong
Design Pressure P_d (MPa)	101.31	67.87	90.50	90.50	105.58
Ultimate Strength P_u (MPa)	110.15	73.61	99.32	99.32	115.37
Design Margin (%)	8.73	8.46	9.74	9.74	9.27

Chapter 6 Conclusions and future work

6.1 Conclusions

This thesis primarily focused on the comparison of the design results of various classification rules. Additionally, it proposed a design method that estimated the scantling of the spherical pressure shell, and conducted simulations to verify the accuracy of the proposed design method. The results of this thesis are summarized as follows:

- (1) The common basis of the classification rules for the design of the spherical pressure shell is the classical yield load formula and the theoretical elastic buckling formula.
- (2) The five pressure shells studied herein were used as the design objects based on which the calculation results were evaluated based on seven classification rules. According to the calculated results of this thesis, the actually used thickness of the existing pressure shell was smaller than the design thickness calculated by most classification rules. The largest deviation was approximately 30%.
- (3) The stress and stability analyses were carried out with the ABAQUS numerical analysis software to discuss the ultimate strength of the pressure shell. After the elastic–plastic buckling analysis, the ultimate strength and collapse modes were obtained and were found to be similar to the test results. This confirmed the increased accuracy of the FE method of this thesis.
- (4) According to the elastic–plastic buckling analysis, it was determined that the existing pressure shell met the design requirements but did not meet the classification rules.
- (5) This thesis proposed that LR rules should be used to evaluate the structural collapse trend and that the correction curve of the BSI specifications should be used for the design correction of the yield load. The usability of the design method was confirmed with FE analyses.
- (6) According to the analysis results, the design method proposed herein can maintain a design margin of about 10% under different pressure shell geometries. This design margin can compensate for the loss that will occur during subsequent maintenance. This method can effectively reduce the thickness of the pressure shell that will in turn reduce its cost and maintain its safety.

- (7) The successful experience of 5 titanium alloy spherical pressure shells exemplified in this thesis shows that such a formula is safe enough for HOV. Most of the current design rules are too conservative. It is recommended to update the core formulas based on the calculation results of this thesis and related formulas.

6.2 Future work

Although this design method proposed by this thesis has yielded good design results in the five pressure shells tested herein, there are still some problems in this area that need to be improved. Details are as follows:

- (4) There are several openings in the spherical pressure shell that weaken its critical strength. In future research, an in-depth study of the opening reinforcement method based on the design method proposed by this thesis.
- (5) In addition to the problem of stress concentration in the opening, the fatigue damage accumulated in the opening is also the focus of the design of the spherical pressure shell. In future studies, the fatigue damage accumulated in each local area should be explored based on the opening reinforcement design to evaluate the fatigue life of the pressure shell. Additionally, compare the reinforcement methods of each opening, it will cause which kind of influence on the fatigue life of pressure shell.
- (6) When manufacturing the spherical pressure shell, it is usually necessary to weld the two hemispherical crowns that have been manufactured. It is also extremely important to study the influence of the residual stress at the welding seam of the spherical shell on the ultimate strength of the pressure-resistant spherical shell.

Appendix

Appendix I Design of spherical pressure shell (Shinkai 6500)

	Design of Spherical Pressure Shell	Rev. 0 2019/2/26																																																	
		Rev. 1 2019/3/31																																																	
		Rev. 2 2020/6/2																																																	
Symbol	Definition	Unit	Data																																																
Material	Ti-6Al-4V (Min)																																																		
σ_y	The yield strength of material	Mpa	790																																																
E	The young's modulus of material	Mpa	113800																																																
ν	The poisson's ratio of material		0.342																																																
D_i	The inner diameter of shell	mm	2000																																																
MOD	The maximum operating depth	m	6500																																																
P	The maximum operating pressure	MPa	65.36																																																
sf	Safety factor for design		1.55																																																
Pd	$P \cdot sf$	MPa	101.31																																																
<table> <tr> <th>Material</th><th>σ_y (MPa)</th><th>E (MPa)</th><th></th></tr> <tr> <td>HY-80</td><td>550</td><td>207000</td><td>MIL</td></tr> <tr> <td>HY-100</td><td>690</td><td>207000</td><td>MIL</td></tr> <tr> <td>HSLA-80</td><td>552</td><td>205000</td><td>CR</td></tr> <tr> <td>HSLA-100($\leq 102\text{mm}$)</td><td>690</td><td>205000</td><td>CR</td></tr> <tr> <td>HSLA-100($> 102\text{mm}$)</td><td>655</td><td>205000</td><td>CR</td></tr> <tr> <td>Fe-510</td><td>355</td><td>206000</td><td>ISO</td></tr> <tr> <td>AH/EH/DH32</td><td>315</td><td>206000</td><td>ABS</td></tr> <tr> <td>AH/EH/DH36</td><td>355</td><td>206000</td><td>ABS</td></tr> <tr> <td>Ti-6Al-4V (Min)</td><td>872</td><td>114800</td><td>AMS</td></tr> <tr> <td>Ti-6Al-4V ELI</td><td>790</td><td>113800</td><td>AMS</td></tr> <tr> <td>Ti-6211</td><td>790</td><td>115000</td><td>AMS</td></tr> </table>				Material	σ_y (MPa)	E (MPa)		HY-80	550	207000	MIL	HY-100	690	207000	MIL	HSLA-80	552	205000	CR	HSLA-100($\leq 102\text{mm}$)	690	205000	CR	HSLA-100($> 102\text{mm}$)	655	205000	CR	Fe-510	355	206000	ISO	AH/EH/DH32	315	206000	ABS	AH/EH/DH36	355	206000	ABS	Ti-6Al-4V (Min)	872	114800	AMS	Ti-6Al-4V ELI	790	113800	AMS	Ti-6211	790	115000	AMS
Material	σ_y (MPa)	E (MPa)																																																	
HY-80	550	207000	MIL																																																
HY-100	690	207000	MIL																																																
HSLA-80	552	205000	CR																																																
HSLA-100($\leq 102\text{mm}$)	690	205000	CR																																																
HSLA-100($> 102\text{mm}$)	655	205000	CR																																																
Fe-510	355	206000	ISO																																																
AH/EH/DH32	315	206000	ABS																																																
AH/EH/DH36	355	206000	ABS																																																
Ti-6Al-4V (Min)	872	114800	AMS																																																
Ti-6Al-4V ELI	790	113800	AMS																																																
Ti-6211	790	115000	AMS																																																

Appendix

e : The minimum calculated thickness of shell plate

$$e = \frac{PR_m}{2t} = \frac{PR_i}{(4\sigma_y - p)} = \underline{\quad 21.12 \quad} \text{ mm}$$

P_e : The elastic instability pressure for collapse of spherical shell

$$P_e = \frac{1.21 E e^2}{R_m^2}$$

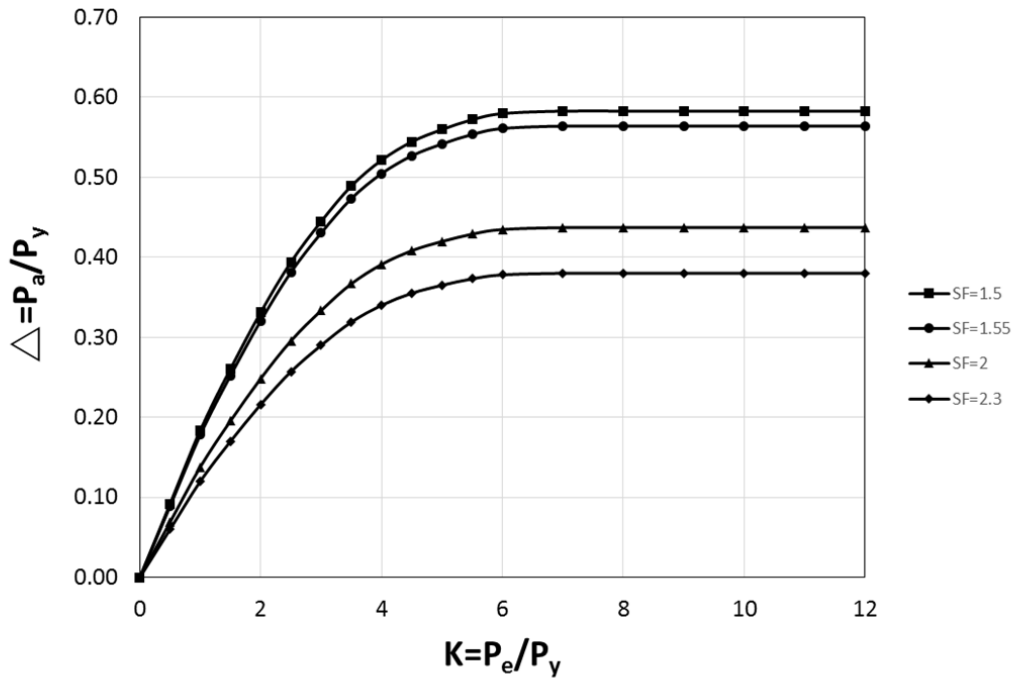
P_{yss} : The pressure at which membrane stress in spherical shell reaches the yield point of material

$$P_{yss} = \frac{2\sigma_y t}{R_m} \quad P_{ys} = \frac{\gamma_m}{sf} P_y$$

P_a : The calculated allowable external pressure

Δ , K : Parameter used in calculating the required external design pressure

$$\Delta = \frac{1}{\sqrt{1 + \left(\frac{1}{0.3K}\right)^2 \cdot S.F.}} = \frac{P_a}{P_{yss}} \quad K = \frac{P_e}{P_{yss}}$$



Appendix

Assume					
$\sigma_y =$	790	790	790	790	790
Multiple =	1.5	2.3	3.0	3.8	4.5
$e =$	31.68	47.52	63.36	79.20	95.04
$R =$	1015.8	1023.8	1031.7	1039.6	1047.5
$p_e =$	133.92	296.68	519.36	799.19	1133.50
$p_{yss} =$	49.27	73.34	97.04	120.37	143.35
$K =$	2.72	4.05	5.35	6.64	7.91
$\Delta =$	0.526	0.565	0.585	0.597	0.604
$P_a =$	25.94	41.47	56.76	71.81	86.64

N/mm² (Mpa)

mm

mm

N/mm² (Mpa)

N/mm² (Mpa)

N/mm² (Mpa)

Interpolating p_a versus e for the design external pressure p gives $e = \underline{72.41}$ mm

$e_{act} = \underline{72.40}$ mm

Design Case

When design external pressure $P = \underline{65.359}$ N/mm² (Mpa)

$e = \underline{72.400}$ mm

$R = \underline{1036.2}$ mm

$p_{yss} = \underline{110.4}$ N/mm² (Mpa)

$p_e = \underline{672.2}$ N/mm² (Mpa)

$K = \underline{6.1}$

$\Delta = \underline{0.592}$

$P_a = \underline{65.4}$ N/mm² (Mpa)

CHECK $P_a \geq P$

OK

* Calculate the allowable external pressure p_a . If this value is less than the design external pressure p , the assumed value of e shall be **increased until p_a is greater than or equal to p .**

Appendix

Appendix II Design of spherical pressure shell (Alvin)

	Design of Spherical Pressure Shell	Rev. 0	2019/2/26																																																
		Rev. 1	2019/3/31																																																
	Alvin	Rev. 2	2020/6/2																																																
Symbol	Definition	Unit	Data																																																
Material	Ti-6Al-4V (Min)																																																		
σ_y	The yield strength of material	Mpa	790																																																
E	The young's modulus of material	Mpa	115000																																																
ν	The poisson's ratio of material		0.31																																																
D_i	The inner diameter of shell	mm	2000																																																
MOD	The maximum operating depth	m	4500																																																
P	The maximum operating pressure	MPa	45.25																																																
sf	Safety factor for design		1.50																																																
Pd	P*sf	MPa	67.87																																																
<table> <tr> <th>Material</th><th>σ_y (MPa)</th><th>E (MPa)</th><th></th></tr> <tr> <td>HY-80</td><td>550</td><td>207000</td><td>MIL</td></tr> <tr> <td>HY-100</td><td>690</td><td>207000</td><td>MIL</td></tr> <tr> <td>HSLA-80</td><td>552</td><td>205000</td><td>CR</td></tr> <tr> <td>HSLA-100(≤ 102mm)</td><td>690</td><td>205000</td><td>CR</td></tr> <tr> <td>HSLA-100(> 102mm)</td><td>655</td><td>205000</td><td>CR</td></tr> <tr> <td>Fe-510</td><td>355</td><td>206000</td><td>ISO</td></tr> <tr> <td>AH/EH/DH32</td><td>315</td><td>206000</td><td>ABS</td></tr> <tr> <td>AH/EH/DH36</td><td>355</td><td>206000</td><td>ABS</td></tr> <tr> <td>Ti-6Al-4V (Min)</td><td>872</td><td>114800</td><td>AMS</td></tr> <tr> <td>Ti-6Al-4V ELI</td><td>790</td><td>113800</td><td>AMS</td></tr> <tr> <td>Ti-6211</td><td>790</td><td>115000</td><td>AMS</td></tr> </table>				Material	σ_y (MPa)	E (MPa)		HY-80	550	207000	MIL	HY-100	690	207000	MIL	HSLA-80	552	205000	CR	HSLA-100(≤ 102 mm)	690	205000	CR	HSLA-100(> 102 mm)	655	205000	CR	Fe-510	355	206000	ISO	AH/EH/DH32	315	206000	ABS	AH/EH/DH36	355	206000	ABS	Ti-6Al-4V (Min)	872	114800	AMS	Ti-6Al-4V ELI	790	113800	AMS	Ti-6211	790	115000	AMS
Material	σ_y (MPa)	E (MPa)																																																	
HY-80	550	207000	MIL																																																
HY-100	690	207000	MIL																																																
HSLA-80	552	205000	CR																																																
HSLA-100(≤ 102 mm)	690	205000	CR																																																
HSLA-100(> 102 mm)	655	205000	CR																																																
Fe-510	355	206000	ISO																																																
AH/EH/DH32	315	206000	ABS																																																
AH/EH/DH36	355	206000	ABS																																																
Ti-6Al-4V (Min)	872	114800	AMS																																																
Ti-6Al-4V ELI	790	113800	AMS																																																
Ti-6211	790	115000	AMS																																																

Appendix

e : The minimum calculated thickness of shell plate

$$e = \frac{PR_m}{2t} = \frac{PR_i}{(4\sigma_y - p)} = \underline{\quad 14.53 \quad} \text{ mm}$$

P_e : The elastic instability pressure for collapse of spherical shell

$$P_e = \frac{1.21 E e^2}{R_m^2}$$

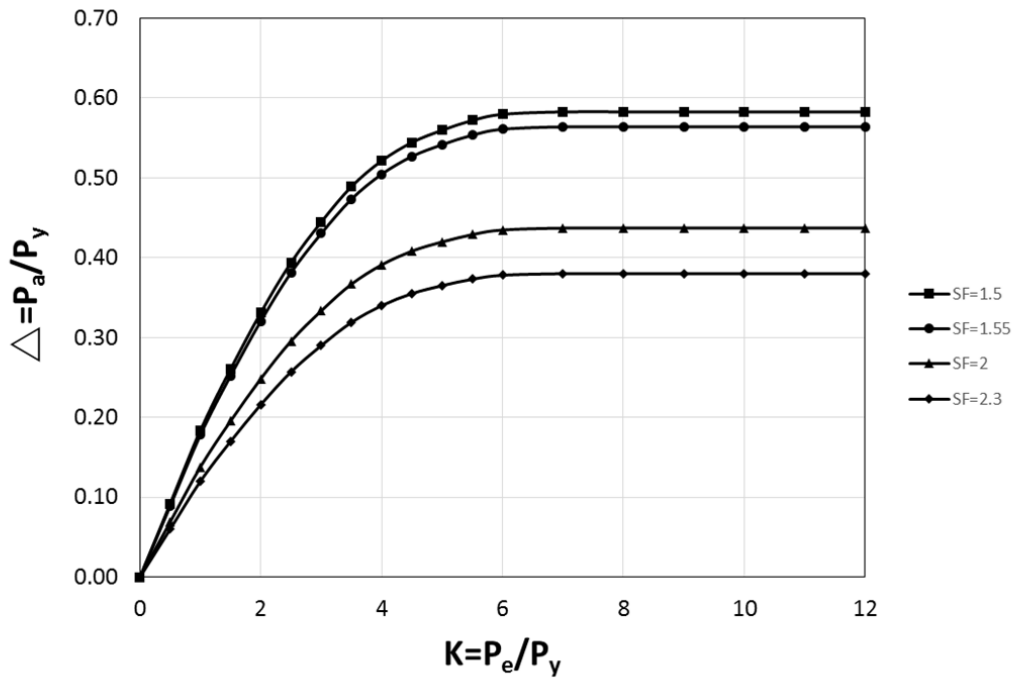
P_{yss} : The pressure at which membrane stress in spherical shell reaches the yield point of material

$$P_{yss} = \frac{2\sigma_y t}{R_m}$$

P_a : The calculated allowable external pressure

Δ , K : Parameter used in calculating the required external design pressure

$$\Delta = \frac{1}{\sqrt{1 + \left(\frac{1}{0.3K}\right)^2 \cdot S.F.}} = \frac{P_a}{P_{yss}} \quad K = \frac{P_e}{P_{yss}}$$



Appendix

Assume					
$\sigma_y =$	790	790	790	790	790
Multiple =	1.5	2.3	3.0	3.8	4.5
$e =$	21.79	32.69	43.58	54.48	65.37
$R =$	1010.9	1016.3	1021.8	1027.2	1032.7
$p_e =$	64.66	143.92	253.14	391.35	557.62
$p_{yss} =$	34.06	50.81	67.39	83.79	100.02
$K =$	1.90	2.83	3.76	4.67	5.58
$\Delta =$	0.491	0.549	0.578	0.595	0.607
$P_a =$	16.73	27.90	38.95	49.88	60.70

N/mm² (Mpa)

mm

mm

N/mm² (Mpa)

N/mm² (Mpa)

N/mm² (Mpa)

Interpolating p_a versus e for the design external pressure , gives $e = \underline{49.86}$ mm

$e_{act} = \underline{49.90}$ mm

Design Case

When design external pressure $P = \underline{45.249}$ N/mm² (Mpa)

$e = \underline{49.900}$ mm

$R = \underline{1025.0}$ mm

$p_{yss} = \underline{76.9}$ N/mm² (Mpa)

$p_e = \underline{329.8}$ N/mm² (Mpa)

$K = \underline{4.3}$

$\Delta = \underline{0.6}$

$P_a = \underline{45.3}$ N/mm² (Mpa)

CHECK $P_a \geq P$

OK

* Calculate the allowable external pressure p_a . If this value is less than the design external pressure p , the assumed value of e shall be **increased until p_a is greater than or equal to p .**

Appendix

Appendix III Design of spherical pressure shell (Nautil)

	Design of Spherical Pressure Shell	Rev. 0	2019/2/26																																																
		Rev. 1	2019/3/31																																																
	Nautil	Rev. 2	2020/6/2																																																
Symbol	Definition	Unit	Data																																																
Material	Ti-6Al-4V (Min)																																																		
σ_y	The yield strength of material	Mpa	872																																																
E	The young's modulus of material	Mpa	114800																																																
ν	The poisson's ratio of material		0.33																																																
D_i	The inner diameter of shell	mm	2100																																																
MOD	The maximum operating depth	m	6000																																																
P	The maximum operating pressure	MPa	60.33																																																
sf	Safety factor for design		1.50																																																
Pd	P*sf	MPa	90.50																																																
<table> <tr> <th>Material</th><th>σ_y (MPa)</th><th>E (MPa)</th><th></th></tr> <tr> <td>HY-80</td><td>550</td><td>207000</td><td>MIL</td></tr> <tr> <td>HY-100</td><td>690</td><td>207000</td><td>MIL</td></tr> <tr> <td>HSLA-80</td><td>552</td><td>205000</td><td>CR</td></tr> <tr> <td>HSLA-100(≤ 102mm</td><td>690</td><td>205000</td><td>CR</td></tr> <tr> <td>HSLA-100(> 102mm</td><td>655</td><td>205000</td><td>CR</td></tr> <tr> <td>Fe-510</td><td>355</td><td>206000</td><td>ISO</td></tr> <tr> <td>AH/EH/DH32</td><td>315</td><td>206000</td><td>ABS</td></tr> <tr> <td>AH/EH/DH36</td><td>355</td><td>206000</td><td>ABS</td></tr> <tr> <td>Ti-6Al-4V (Min)</td><td>872</td><td>114800</td><td>AMS</td></tr> <tr> <td>Ti-6Al-4V ELI</td><td>790</td><td>113800</td><td>AMS</td></tr> <tr> <td>Ti-6211</td><td>790</td><td>115000</td><td>AMS</td></tr> </table>				Material	σ_y (MPa)	E (MPa)		HY-80	550	207000	MIL	HY-100	690	207000	MIL	HSLA-80	552	205000	CR	HSLA-100(≤ 102 mm	690	205000	CR	HSLA-100(> 102 mm	655	205000	CR	Fe-510	355	206000	ISO	AH/EH/DH32	315	206000	ABS	AH/EH/DH36	355	206000	ABS	Ti-6Al-4V (Min)	872	114800	AMS	Ti-6Al-4V ELI	790	113800	AMS	Ti-6211	790	115000	AMS
Material	σ_y (MPa)	E (MPa)																																																	
HY-80	550	207000	MIL																																																
HY-100	690	207000	MIL																																																
HSLA-80	552	205000	CR																																																
HSLA-100(≤ 102 mm	690	205000	CR																																																
HSLA-100(> 102 mm	655	205000	CR																																																
Fe-510	355	206000	ISO																																																
AH/EH/DH32	315	206000	ABS																																																
AH/EH/DH36	355	206000	ABS																																																
Ti-6Al-4V (Min)	872	114800	AMS																																																
Ti-6Al-4V ELI	790	113800	AMS																																																
Ti-6211	790	115000	AMS																																																

Appendix

e : The minimum calculated thickness of shell plate

$$e = \frac{PR_m}{2t} = \frac{PR_i}{(4\sigma_y - p)} = \underline{\underline{18.48}} \text{ mm}$$

P_e : The elastic instability pressure for collapse of spherical shell

$$P_e = \frac{1.21 E e^2}{R_m^2}$$

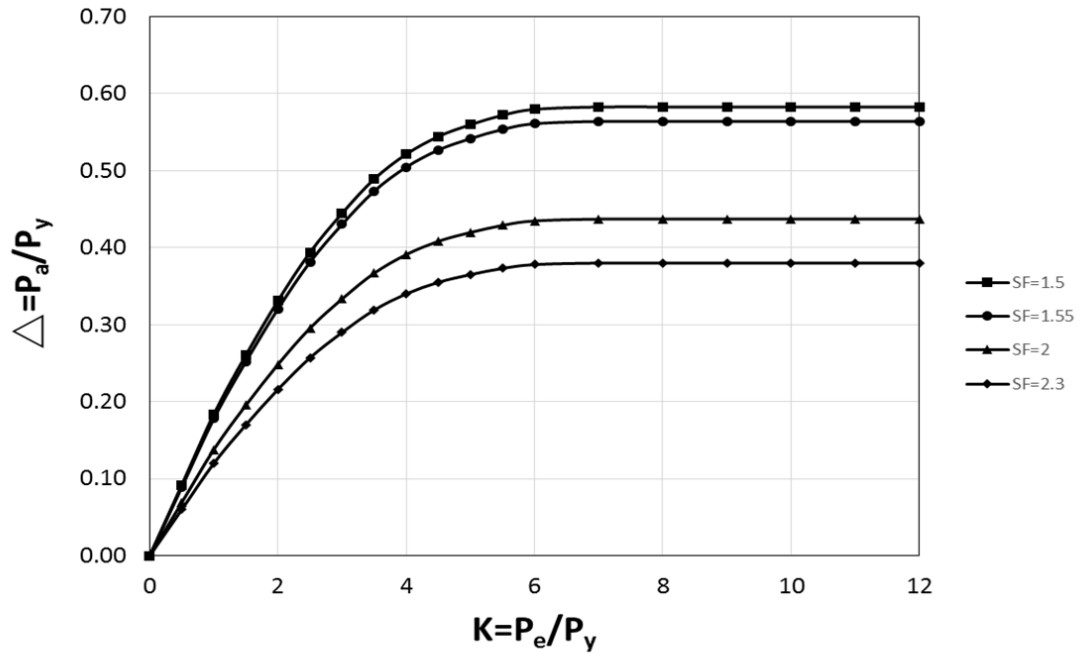
P_{yss} : The pressure at which membrane stress in spherical shell reaches the yield point of material

$$P_{yss} = \frac{2\sigma_y t}{R_m}$$

P_a : The calculated allowable external pressure

Δ 、 K : Parameter used in calculating the required external design pressure

$$\Delta = \frac{1}{\sqrt{1 + \left(\frac{1}{0.3K}\right)^2 \cdot S.F.}} = \frac{P_a}{P_{yss}} \quad K = \frac{P_e}{P_{yss}}$$



Appendix

Assume					
$\sigma_y =$	872	872	872	872	872
Multiple =	1.5	2.3	3.0	3.8	4.5
$e =$	27.72	41.58	55.44	69.31	83.17
$R =$	1063.9	1070.8	1077.7	1084.7	1091.6
$p_e =$	94.32	209.48	367.64	567.12	806.32
$p_{yss} =$	45.45	67.73	89.72	111.44	132.87
$K =$	2.08	3.09	4.10	5.09	6.07
$\Delta =$	0.506	0.559	0.585	0.601	0.612
$P_a =$	23.00	37.85	52.52	66.99	81.28
					N/mm ² (Mpa)

Interpolating p_a versus e for the design external pressure , gives $e = \underline{62.93}$ mm

$e_{act} = \underline{63.10}$ mm

Design Case

When design external pressure $P = \underline{60.332}$ N/mm² (Mpa)

$e = \underline{63.100}$ mm

$R = \underline{1081.6}$ mm

$p_{yss} = \underline{101.7}$ N/mm² (Mpa)

$p_e = \underline{472.8}$ N/mm² (Mpa)

$K = \underline{4.6}$

$\Delta = \underline{0.6}$

$P_a = \underline{60.5}$ N/mm² (Mpa)

CHECK $P_a \geq P$

OK

* Calculate the allowable external pressure p_a . If this value is less than the design external pressure p , the assumed value of e shall be **increased until p_a is greater than or equal to p .**

Appendix

Appendix IV Design of spherical pressure shell (Consul)

	Design of Spherical Pressure Shell	Rev. 0	2019/2/26																																																
		Rev. 1	2019/3/31																																																
	Consul	Rev. 2	2020/6/2																																																
Symbol	Definition	Unit	Data																																																
Material	Ti-6Al-4V (Min)																																																		
σ_y	The yield strength of material	Mpa	872																																																
E	The young's modulus of material	Mpa	114800																																																
ν	The poisson's ratio of material		0.33																																																
D_i	The inner diameter of shell	mm	2100																																																
MOD	The maximum operating depth	m	6000																																																
P	The maximum operating pressure	MPa	60.33																																																
sf	Safety factor for design		1.50																																																
Pd	P*sf	MPa	90.50																																																
<table> <tr> <th>Material</th><th>σ_y (MPa)</th><th>E (MPa)</th><th></th></tr> <tr> <td>HY-80</td><td>550</td><td>207000</td><td>MIL</td></tr> <tr> <td>HY-100</td><td>690</td><td>207000</td><td>MIL</td></tr> <tr> <td>HSLA-80</td><td>552</td><td>205000</td><td>CR</td></tr> <tr> <td>HSLA-100(≤ 102mm</td><td>690</td><td>205000</td><td>CR</td></tr> <tr> <td>HSLA-100(> 102mm</td><td>655</td><td>205000</td><td>CR</td></tr> <tr> <td>Fe-510</td><td>355</td><td>206000</td><td>ISO</td></tr> <tr> <td>AH/EH/DH32</td><td>315</td><td>206000</td><td>ABS</td></tr> <tr> <td>AH/EH/DH36</td><td>355</td><td>206000</td><td>ABS</td></tr> <tr> <td>Ti-6Al-4V (Min)</td><td>872</td><td>114800</td><td>AMS</td></tr> <tr> <td>Ti-6Al-4V ELI</td><td>790</td><td>113800</td><td>AMS</td></tr> <tr> <td>Ti-6211</td><td>790</td><td>115000</td><td>AMS</td></tr> </table>				Material	σ_y (MPa)	E (MPa)		HY-80	550	207000	MIL	HY-100	690	207000	MIL	HSLA-80	552	205000	CR	HSLA-100(≤ 102 mm	690	205000	CR	HSLA-100(> 102 mm	655	205000	CR	Fe-510	355	206000	ISO	AH/EH/DH32	315	206000	ABS	AH/EH/DH36	355	206000	ABS	Ti-6Al-4V (Min)	872	114800	AMS	Ti-6Al-4V ELI	790	113800	AMS	Ti-6211	790	115000	AMS
Material	σ_y (MPa)	E (MPa)																																																	
HY-80	550	207000	MIL																																																
HY-100	690	207000	MIL																																																
HSLA-80	552	205000	CR																																																
HSLA-100(≤ 102 mm	690	205000	CR																																																
HSLA-100(> 102 mm	655	205000	CR																																																
Fe-510	355	206000	ISO																																																
AH/EH/DH32	315	206000	ABS																																																
AH/EH/DH36	355	206000	ABS																																																
Ti-6Al-4V (Min)	872	114800	AMS																																																
Ti-6Al-4V ELI	790	113800	AMS																																																
Ti-6211	790	115000	AMS																																																

Appendix

e : The minimum calculated thickness of shell plate

$$e = \frac{PR_m}{2t} = \frac{PR_i}{(4\sigma_y - p)} = \underline{\underline{18.48}} \text{ mm}$$

P_e : The elastic instability pressure for collapse of spherical shell

$$P_e = \frac{1.21 E e^2}{R_m^2}$$

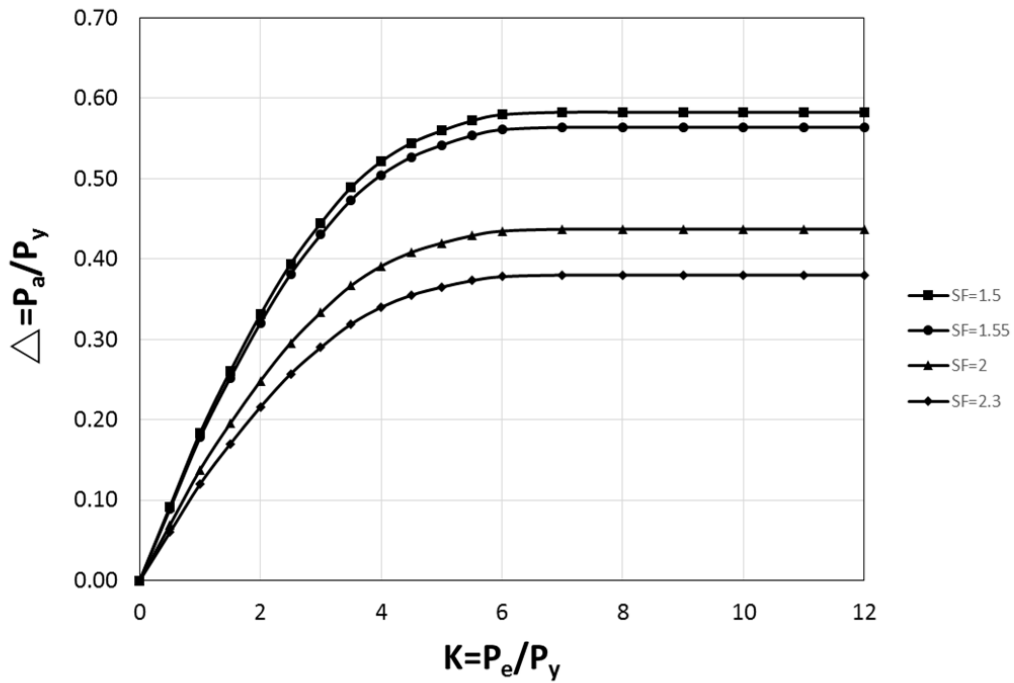
P_{yss} : The pressure at which membrane stress in spherical shell reaches the yield point of material

$$P_{yss} = \frac{2\sigma_y t}{R_m}$$

P_a : The calculated allowable external pressure

Δ , K : Parameter used in calculating the required external design pressure

$$\Delta = \frac{1}{\sqrt{1 + \left(\frac{1}{0.3K}\right)^2 \cdot S.F.}} = \frac{P_a}{P_{yss}} \quad K = \frac{P_e}{P_{yss}}$$



Appendix

Assume					
$\sigma_y =$	872	872	872	872	872
Multiple =	1.5	2.3	3.0	3.8	4.5
$e =$	27.72	41.58	55.44	69.31	83.17
$R =$	1063.9	1070.8	1077.7	1084.7	1091.6
$p_e =$	94.32	209.48	367.64	567.12	806.32
$p_{yss} =$	45.45	67.73	89.72	111.44	132.87
$K =$	2.08	3.09	4.10	5.09	6.07
$\Delta =$	0.506	0.559	0.585	0.601	0.612
$P_a =$	23.00	37.85	52.52	66.99	81.28

N/mm² (Mpa)

mm

mm

N/mm² (Mpa)

N/mm² (Mpa)

N/mm² (Mpa)

Interpolating p_a versus e for the design external pressure , gives $e =$ 62.93 mm

$e_{act} =$ 63.10 mm

Design Case

When design external pressure $P =$ 60.332 N/mm² (Mpa)

$e =$ 63.100 mm

$R =$ 1081.6 mm

$p_{yss} =$ 101.7 N/mm² (Mpa)

$p_e =$ 472.8 N/mm² (Mpa)

$K =$ 4.6

$\Delta =$ 0.6

$P_a =$ 60.5 N/mm² (Mpa)

CHECK $P_a \geq P$

OK

* Calculate the allowable external pressure p_a . If this value is less than the design external pressure p , the assumed value of e shall be **increased until p_a is greater than or equal to p .**

Appendix

Appendix V Design of spherical pressure shell (Jiaolong)

	Design of Spherical Pressure Shell	Rev. 0	2019/2/26																																																
		Rev. 1	2019/3/31																																																
	Jiaolong	Rev. 2	2020/6/2																																																
Symbol	Definition	Unit	Data																																																
Material	Ti-6Al-4V (Min)																																																		
σ_y	The yield strength of material	Mpa	872																																																
E	The young's modulus of material	Mpa	114800																																																
ν	The poisson's ratio of material		0.33																																																
D_i	The inner diameter of shell	mm	2100																																																
MOD	The maximum operating depth	m	7000																																																
P	The maximum operating pressure	MPa	70.39																																																
sf	Safety factor for design		1.50																																																
Pd	P*sf	MPa	105.58																																																
<table> <tr> <th>Material</th><th>σ_y (MPa)</th><th>E (MPa)</th><th></th></tr> <tr> <td>HY-80</td><td>550</td><td>207000</td><td>MIL</td></tr> <tr> <td>HY-100</td><td>690</td><td>207000</td><td>MIL</td></tr> <tr> <td>HSLA-80</td><td>552</td><td>205000</td><td>CR</td></tr> <tr> <td>HSLA-100(≤ 102mm)</td><td>690</td><td>205000</td><td>CR</td></tr> <tr> <td>HSLA-100(> 102mm)</td><td>655</td><td>205000</td><td>CR</td></tr> <tr> <td>Fe-510</td><td>355</td><td>206000</td><td>ISO</td></tr> <tr> <td>AH/EH/DH32</td><td>315</td><td>206000</td><td>ABS</td></tr> <tr> <td>AH/EH/DH36</td><td>355</td><td>206000</td><td>ABS</td></tr> <tr> <td>Ti-6Al-4V (Min)</td><td>872</td><td>114800</td><td>AMS</td></tr> <tr> <td>Ti-6Al-4V ELI</td><td>790</td><td>113800</td><td>AMS</td></tr> <tr> <td>Ti-6211</td><td>790</td><td>115000</td><td>AMS</td></tr> </table>				Material	σ_y (MPa)	E (MPa)		HY-80	550	207000	MIL	HY-100	690	207000	MIL	HSLA-80	552	205000	CR	HSLA-100(≤ 102 mm)	690	205000	CR	HSLA-100(> 102 mm)	655	205000	CR	Fe-510	355	206000	ISO	AH/EH/DH32	315	206000	ABS	AH/EH/DH36	355	206000	ABS	Ti-6Al-4V (Min)	872	114800	AMS	Ti-6Al-4V ELI	790	113800	AMS	Ti-6211	790	115000	AMS
Material	σ_y (MPa)	E (MPa)																																																	
HY-80	550	207000	MIL																																																
HY-100	690	207000	MIL																																																
HSLA-80	552	205000	CR																																																
HSLA-100(≤ 102 mm)	690	205000	CR																																																
HSLA-100(> 102 mm)	655	205000	CR																																																
Fe-510	355	206000	ISO																																																
AH/EH/DH32	315	206000	ABS																																																
AH/EH/DH36	355	206000	ABS																																																
Ti-6Al-4V (Min)	872	114800	AMS																																																
Ti-6Al-4V ELI	790	113800	AMS																																																
Ti-6211	790	115000	AMS																																																

Appendix

e : The minimum calculated thickness of shell plate

$$e = \frac{PR_m}{2t} = \frac{PR_i}{(4\sigma_y - p)} = \underline{\underline{21.63}} \text{ mm}$$

P_e : The elastic instability pressure for collapse of spherical shell

$$P_e = \frac{1.21 E e^2}{R_m^2}$$

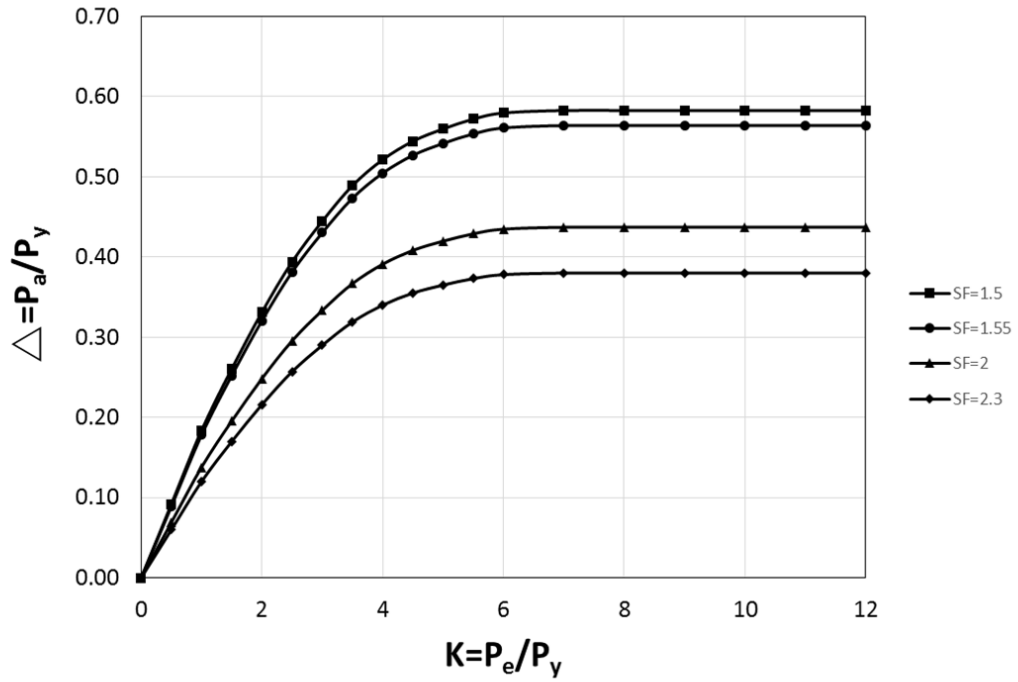
P_{yss} : The pressure at which membrane stress in spherical shell reaches the yield point of material

$$P_{yss} = \frac{2\sigma_y t}{R_m}$$

P_a : The calculated allowable external pressure

Δ 、 K : Parameter used in calculating the required external design pressure

$$\Delta = \frac{1}{\sqrt{1 + \left(\frac{1}{0.3K}\right)^2 \cdot S.F.}} = \frac{P_a}{P_{yss}} \quad K = \frac{P_e}{P_{yss}}$$



Appendix

Assume					
$\sigma_y =$	872	872	872	872	872
Multiple =	1.5	2.3	3.0	3.8	4.5
$e =$	32.44	48.66	64.88	81.09	97.31
$R =$	1066.2	1074.3	1082.4	1090.5	1098.7
$p_e =$	128.57	284.93	498.97	768.10	1089.79
$p_{yss} =$	53.06	78.99	104.53	129.69	154.47
$K =$	2.42	3.61	4.77	5.92	7.05
$\Delta =$	0.529	0.574	0.597	0.610	0.619
$P_a =$	28.07	45.36	62.38	79.16	95.68

N/mm² (Mpa)

mm

mm

N/mm² (Mpa)

N/mm² (Mpa)

N/mm² (Mpa)

Interpolating p_a versus e for the design external pressure p gives $e = \underline{72.61}$ mm

$e_{act} = \underline{72.80}$ mm

Design Case

When design external pressure $P = \underline{70.387}$ N/mm² (Mpa)

$e = \underline{72.800}$ mm

$R = \underline{1086.4}$ mm

$p_{yss} = \underline{116.9}$ N/mm² (Mpa)

$p_e = \underline{623.7}$ N/mm² (Mpa)

$K = \underline{5.3}$

$\Delta = \underline{0.6}$

$P_a = \underline{70.6}$ N/mm² (Mpa)

CHECK $P_a \geq P$

OK

* Calculate the allowable external pressure p_a . If this value is less than the design external pressure p , the assumed value of e shall be **increased until p_a is greater than or equal to p .**

Acknowledgment

Studying for a PhD is a truly life-changing experience for me, and it is also the first time I have left my country to live alone. Without the support and guidance, I got from many people, I think this would be impossible.

I would like to first say a very big thank you to my advisor Prof. Kiyokazu Minami, for all the support and encouragement he gave me at Tokyo University of Marine Science and Technology. Without his guidance and constant feedback this PhD would not have been achievable. I could not have imagined having a better advisor and mentor for my PhD study. When I first came to a strange country, the language barrier brought a lot of inconvenience to daily life and study. It was the professor Minami who kept caring about me and gave me a lot of help, allowing me to adapt to life and study in Japan.

Besides my advisor, I would like to thank the rest of my thesis committee: Prof. Masuda and Prof. Kondo, for giving me a lot of advice. With their insightful comments and encouragement, they have inspired me to conduct research from all angles and made the paper more rich and powerful.

However, without the support of the scholarship program of the Japan-Taiwan Exchange Association, I would not be able to concentrate on my research without worry. I would like to express my sincere gratitude to the association.

The long student life is coming to an end. I must thank many people who helped me along the way. During my Japanese learning process, Prof. Nabatame gave me a lot of help. My friends who in Taiwan, regardless of my sorrows and joys, they have always been with me. Here I would like to express my sincere gratitude to everyone for your company.

Last but not the least, I would like to thank my family: my parents and my sisters for supporting me spiritually throughout writing this thesis and my life in general. Although I can't always be with them, they still support and respect every decision I make. Finally, hope my family is healthy and happy.

HUANG YUNGHSIN
September 2021
Tokyo, Japan